

台灣中央山脈東翼玉里帶及板岩帶掘升倒轉及變形歷史研究

楊凱翔¹、李建成²、陳于高¹、何恭睿²

(1)臺灣大學地質科學研究所、(2)中央研究院地球科學研究所

本研究的目的是，為了更適切地了解台灣中央山脈東翼造山的過程，特別是整個中央山脈發育的扇狀劈理，及中後楔(retro-wedge)的掘升過程。近期的研究指出，中央山脈東翼的玉里帶主要的劈理，可能是在隱沒過程中經歷溫壓峰值 (Peak P/T) 所形成，爾後在掘升(exhumation)過程中，造成了劈理倒轉的現象。在本研究中，我們對沿鹿寮溪及鹿野溪進行了野外調查和薄片分析觀察，並結合近幾年發表的 RSCM 變質溫度，和鉛石鈾鉛定年的資料，提供中央山脈東翼玉里帶及其上覆的板岩帶之構造演化的解釋。

綜合野外調查及薄片觀察的結果，我們將變形作用分為兩期：D1 與 D2，及對應形成的劈理 (S1、S2)。劈理的特徵及位態由西向東的分佈如下：

在玉里帶中的石英雲母片岩，在西側主要是 S0/S1 形成的「向西伸向不對稱褶皺」，及覆蓋其上的「向西傾 (40°-70°) 穿透性最強的 S2」；而玉里帶東側的雲母片岩 (也稱初來層)，主要是 S0/S1 形成的「向東的伸向不對稱褶皺」，及覆蓋其上「向西傾 S2 (30°-40°)」，且 S2 傾角由西向東似乎呈現逐漸變緩的趨勢外，伴隨左移的剪切的伸張線理(220, 10)。

在沈積時期，玉里帶上覆的板岩帶，為中新世隱沒濁流岩中最年輕的地層。其變質度的範圍涵括了由片岩過渡到變質砂岩、千枚岩漸變至板岩。板岩帶在東西向剖面呈現一向西伸向的不對稱褶皺 F1 與伴隨而生的 S1 劈理。在 F1 軸部常可觀察到複褶皺，在翼部則偶可發現發育後期褶皺急折帶 F2 及對應的 S2 劈理，由於是局部發育，顯示 F2 褶皺及 S2 劈理發育的過程，板岩與玉里帶比較是處在相對低溫的環境；而在南北向剖面的褶皺則發育出後期(secondary)的劈理。

在薄片分析結果，玉里帶的早期劈理 S1，明顯的被穿透性的 S2 截穿，在垂直 S2 面 (XZ 面) 觀察到左移剪切；而板岩帶在 S1 褶皺軸部偶有後期的 S2 劈理發育，而 S1 面發育右剪的黃鐵礦型態壓影構造，垂直 S1 面 (XZ 面) 以純剪伸張為主。

綜合構造分析及其他年代學結果，本研究提出以下中央山脈東翼的構造演化。從玉里帶在隱沒初期 (~10-7 Ma)，濁流岩產生褶皺 (D1) 並伴隨 S1 劈理發育。爾後玉里帶持續向東隱沒並開始受到菲律賓海板塊的聚合擠壓 (~7-5 Ma)，產生了第二期的褶皺(D2)，並伴隨了第二期 S2 劈理 (向東傾)。同時上覆濁流岩 (板岩帶) 也開始受變形變質作用並發育第一期的褶皺及板劈理 S1。玉里帶和板岩帶兩者對應近年發表 RSCM 峰值溫度(深度)，分別為 450-500°C (15-20 km) 及 300-375°C (10-12 km)。在持續的板塊聚合過程中，玉里帶及板岩帶開始快速掘升伴隨橫向的左移剪切 (3-0 Ma)，並使 S2 由原本向東傾倒轉成向西傾，同時板岩帶 S1 也受擠壓，發育後期的褶皺 (D2) 與伴隨的急折帶。

中文關鍵字：玉里帶、板岩、劈理、掘升倒轉



蓬萊運動，臺灣是否存在雙碰撞（隱沒）帶？

陳文山¹

(1)臺灣大學地質科學系

古生代以來，臺灣一直位在華夏古陸邊緣，歷經數次板塊聚合事件。因此，代表聚合板塊產物的混同層（*mélange*）更成為瞭解臺灣大地構造演化歷史的重要訊息，尤其代表新生代混同層或傾瀉層的利吉層、墾丁層與玉里帶。但是，當對於 *mélange* 成因或定義有不同的解釋時，就會導致解讀大地構造演化產生很大的差異。如 Lu and Hsü (1992)認為廬山板岩帶為板塊碰撞產生的混同層，而提出雙碰撞（隱沒）帶模式，認為蓬萊運動歷經了陸（歐亞板塊）—陸（古臺灣地塊；脊樑山脈）—弧（菲律賓海板塊；海岸山脈）的碰撞，潮州與梨山斷層為兩個板塊的邊界；此模式也得到一些迴響。究竟板岩帶是否為混同層（*tectonic mélange*；Hsü (1974)定義）？哪必須從 *mélange* 定義說起。

Greenly (1919)首度提出 *mélange* 名詞，當時只是針對岩層產狀的定義為“*block-in-matrix*”，但不具成因的定義。許靖華(Hsü, 1974)重塑 *mélange* 定義(義涵了成因的概念)，認為位在現今或古老的隱沒帶與造山帶中，此後 *mélange* 一詞才被地質界廣泛應用。而 Silver and Beutner (1980)將 *mélange* 成因再細分為構造、沉積與衝頂等作用。由於“*block-in-matrix*”產狀經常造成研究者在成因解釋上產生混亂與錯誤解釋，於是 Festa et al. (2010)又將 *mélange* 成因分為幾種類型：崩積層、斷層帶與聚合板塊邊界的產物；但代表聚合板塊邊界的 *mélange* 須具有一種特性，即含外來的海洋板塊岩塊（*ophiolitic blocks*）。

Lu and Hsü (1992)認為廬山板岩帶中含有外來的海洋板塊岩塊，但報導地區（寶來、萬大水庫、啞口）出露的火成岩都呈現層間沉積的岩體，屬於板內噴發玄武岩質火成岩，非為外來的蛇綠岩岩塊。依據 Festa et al. (2010)定義，梨山斷層帶應屬於板塊內斷層（Type 6: *mélange* related to intracontinental deformation）。

晚期中新世以來，蓬萊運動發生弧陸碰撞，玉里帶屬於隱沒帶混同層，利吉混同層屬於碰撞帶混同層，壽豐斷層為歐亞與菲律賓海板塊的隱沒邊界，縱谷斷層為碰撞邊界。

中文關鍵字：混同層、利吉層、墾丁層、蓬萊運動、弧陸碰撞

再論墾丁層形成年代與成因

陳文山¹

(1)臺灣大學地質科學系

墾丁層首先由詹新甫 (1974) 命名，並描述含有外來岩塊，認為是晚中新世造山時期崩積產生的傾瀉層。而墾丁混同層由畢慶昌 (Biq, 1977) 命名，認為在臺灣南部形成雙隱沒帶 (利吉與墾丁混同層)，推測在上-更新世南中國海海殼隱沒產生的。

過去曾於恆春半島進行地質製圖的研究者，皆認為墾丁層與之下石門層或馬鞍山層呈現沉積接觸關係，成因屬於傾瀉層。墾丁層化石研究發現含有上新世 (Huang et al., 1983) 與上-更新世 (黃奇瑜等, 1985; 陳文山, 1992) 時代的化石；但 Pelletier and Stephan (1985) 認為上至更新世化石是污染自鄰近馬鞍山層；認為墾丁層時代應為晚中新世。之後，許多研究者將墾丁層對比至梨山斷層帶的 *mélange* 時 (雙隱沒帶模式)，都是採用墾丁層屬於晚中新世的看法。

本研究團隊利用磷灰石核飛跡年代探討恆春半島造山隆起時期，利用里龍山層砂岩與其中變質砂岩礫石的冷卻年代。由年代已完全被重置的結果，顯示里龍山層沉積之後被埋藏的地溫已高於磷灰石核飛跡定年的封存溫度 ($>135^{\circ}\text{C}$)，推測至少被深埋至 2-4 公里深。磷灰石核飛跡年代為 2.6 至 3.5 百萬年，表示約在晚上新世至早更新世，里龍山層 (恆春半島) 受造山運動影響而開始隆起 (推測地溫略高於 135°C)。因此，從恆春半島造山隆起起始年代來看，顯然墾丁混同層不可能形成於晚中新世，而應在晚上新世至早更新世時期；也印證了墾丁層應是更新世堆積的傾瀉層。而墾丁層也不應該延伸至潮州—梨山斷層，此斷層也不屬於晚中新世的板塊邊界。

中文關鍵字：混同層、傾瀉層、墾丁層、恆春半島、磷灰石核飛跡

臺灣北部脊樑山脈板岩層年代與地體構造演化 -

利用碎屑鋁石鈾鉛定年法

張秋蓮¹、許緯豪¹、陳文山¹

(1)臺灣大學地質科學系

臺灣北部脊樑山脈的大南澳片岩與上覆的板岩層，兩者以不整合（E 礫岩）或斷層接觸，由於化石的缺乏，上覆板岩層的年代仍有爭論。以往認為板岩層的年代最老為中生代，部分學者推測為始新世或中新世。近期的研究顯示不整合面上覆的變質石灰岩層，含有始新世以來的珊瑚化石，顯示不整合面上覆的板岩層，時代應為始新世或年輕於始新世。此外，一般認為臺灣自中生代晚期以來的碎屑性沉積物是由來自西側華南提供的碎屑沉積物推積而成，然而，近期的研究表示 E 礫岩是侵蝕來自東側大南澳片岩和變質花崗岩的碎屑沉積物推積而成。因此，E 礫岩上覆的板岩層的沉積物來源與當時的地體架構是值得重新討論的議題。本研究藉由採集自和平溪上游板岩層中所夾變質砂岩與變質凝灰岩樣本，利用碎屑鋁石鈾鉛定年法，探究板岩層的年代，並藉由碎屑鋁石頻譜討論板岩原岩沉積物的來源，進而描繪古近紀以來臺灣地體架構演變。

利用碎屑鋁石鈾鉛定年法，得到板岩層的碎屑鋁石頻譜結果，分別落在鋁石年齡族群三角圖（ternary diagram）的白堊紀、始新世-漸新世與中新世範圍內，無法呈現確切沉積年代，表示板岩層原岩的沉積物來源不單只源自西側華南，還包括東側大南澳片岩的物源供應。此外，板岩層中所夾的變質凝灰岩層，最年輕峰值為 34.5 ± 0.2 Ma，顯示始新世-漸新世時期的張裂活動伴隨著部分火成活動，且板岩層原岩的沉積時代可能始於此時期。綜合碎屑鋁石鈾鉛定年結果，顯示古近紀早期，發生張裂活動，基盤（大南澳片岩和變質花崗岩）形成地壘高區（古中央山脈），受到侵蝕進而沉積變質礫岩層（E 礫岩），地塹產生納積空間，堆積始新世-漸新世的沉積物，並伴隨著火成岩類的侵入。古近紀晚期至新近紀早期，整個區域受熱沉陷作用而下沉，堆積中新世以來的碎屑性沉積物。

中文關鍵字：大南澳片岩、E 礫岩、板岩層、碎屑鋁石鈾鉛定年

海岸山脈秀姑巒溪剖面八里灣層之鋁石及磷灰石核飛跡定年研究：探

討源區山脈的剝蝕演化

李政熹¹、陳文山¹、黃奕彰¹

(1)臺灣大學地質科學系

中期中新世以來，海岸山脈從板塊隱沒形成的火山弧，演變為弧陸碰撞的構造環境。前人多針對山脈岩層進行熱定年分析來了解造山帶的時空演化，然而隨著山脈不斷抬升剝蝕，早期出露的岩層已成為碎屑沉積物堆積於盆地中。因此本研究針對海岸山脈秀姑巒溪剖面，採集八里灣層的變質砂岩礫石及砂岩同時進行鋁石核飛跡(ZFT)及磷灰石核飛跡(AFT)定年，輔以砂岩岩象分析，探討脊樑山脈的剝蝕及冷卻歷史。本研究共分析六個變質砂岩礫石及四個砂岩，礫石年代能反映山脈中特定岩層的抬升冷卻歷史，而砂岩年代頻譜則記錄著源區不同岩層的冷卻年代及剝蝕演化。礫石定年呈現兩種結果：(1) AFT~1.8-1.6 Ma 完全癒合、ZFT~3.4-3.3 Ma 完全癒合；(2) AFT~1.8-1.6 Ma 完全癒合、ZFT 部分癒合；代表源區至少有兩種不同變質度的岩層出露。然而，本研究發現某些砂岩的 AFT 完全癒合峰值~4.0-3.0 Ma，老於同層位礫石的 AFT 年代~1.8-1.6 Ma，甚至老於該砂岩的 ZFT 完全癒合峰值，推測此異常的 AFT 年代群應是混合自不同岩層的結果(硬頁岩及板岩)。砂岩的 ZFT 及 AFT 頻譜皆含有大量完全癒合及部分癒合的年代峰值，且隨著地層層序向上，癒合年代逐漸年輕且含量漸增，顯示 1.5-0.8 Ma 期間山脈已出露大範圍極低度(硬頁岩)至低度變質岩(板岩)，層序上亦呈現反剝蝕現象。此外，根據礫石 ZFT 及 AFT 所記錄的冷卻路徑，源區的變質砂岩層於 3.0-1.5 Ma 開始加速冷卻(剝蝕)，與盆地沉積速率加快的時間相近；由砂岩 ZFT 完全癒合峰值計算的山脈冷卻時間亦向上逐漸減少，顯示在 5.2-0.8 Ma 期間剝蝕速率不斷加快，即源區山脈未達到穩定態。

中文關鍵字：核飛跡定年、鋁石、磷灰石、八里灣層、脊樑山脈、剝蝕歷史

利用水璉礫岩的砂岩與礫石之核飛跡定年研究探討上- 更新世

脊樑山脈剝蝕歷史

陳彤軒¹、陳文山¹

(1)臺灣大學地質科學系

當山脈碰撞抬升時，造山前緣會逐漸下陷，形成前陸盆地。因此海岸山脈的後前陸盆地於上新世以來持續堆積了厚層的造山帶沉積物，這些沉積物記錄了山脈的剝蝕歷史。本研究目的為利用海岸山脈後前陸盆地的沉積物，以核飛跡定年法研究，探討中部脊樑山脈在造山時期地殼抬升的冷卻歷史，以了解脊樑山脈的剝蝕歷史。本研究的樣本採集自鹽寮坑溪（十號橋），地層為蕃薯寮層和八里灣層，採集砂礫岩層中的變質砂岩礫石和基質的砂岩。蕃薯寮層屬於晚上新世的中-下部深海沖積扇、八里灣層為晚上新世至早更新世深海上部沖積扇，皆來自西側的脊樑山脈。由於前人探討海岸山脈盆地的地溫梯度僅有約 14°C/km，故其核飛跡並不會因深埋作用而被癒合，利用盆地地層中碎屑鋁石和磷灰石的核飛跡年代可以計算脊樑山脈的抬升與剝蝕歷史。

本研究指出蕃薯寮層和八里灣層的磷灰石核飛跡的最年輕峰值介於 6.6 Ma 至 2.1 Ma，越年輕的地層其核飛跡年代也隨之年輕，而鋁石核飛跡皆為部份癒合 (partial annealing)，代表其源區地層並沒受到超過 240 度以上的熱事件。而利用磷灰石和鋁石的核飛跡年代得知於中期上新世開始脊樑山脈的冷卻速率約 52°C/Ma，到了 3 Ma 時再進一步加速冷卻。同時利用磷灰石和鋁石核飛跡可以探討源區的剝蝕岩性，在約 4.4 Ma 時（蕃薯寮層）脊樑山脈開始已經在出露（被剝蝕）極低度變質的硬頁岩岩層，約 3.3 Ma 時（八里灣層）開始出露低度變質岩層（板岩）。

中文關鍵字：核飛跡定年法、剝蝕歷史、海岸山脈、水璉礫岩

Modeling the earthquake source process with Langevin's approach

Tsung-Hsi Wu¹、Chien-Chih Chen²

(1)Department of Earth Sciences, National Central University、(2)Department of Earth Sciences,
National Central University; Earthquake-Disaster and Risk Evaluation and Management Center,
National Central University

When dealing with the dynamics in an asymmetric many-body system, analytical solutions are practically unattainable and numerical solutions usually exhibit chaotic behaviors, if interactions between bodies are in concern. To deal with this conundrum, stochastic approaches have been widely applied in modeling the dynamics of many-body systems. Following Langevin's approach, we propose a stochastic dynamic model for the earthquake rupture process where the many degrees of freedom is omitted by introducing the random force that accounts for the collision of structures and uncertainties in the heterogeneity of faulting planes. The model is a one-dimensional Langevin equation of Coulomb friction. It allows fast numerical simulations, and analytical solutions are attainable under the steady-state approximation. Both analytical and numerical results coincide with the truncated exponential (TEX) distribution that is empirically characterized in the rupture models of large earthquake events worldwide, and we relate the scale parameter in the TEX model to the ratio of the driving force and the friction parameter in the Langevin equation given the same noise level. Furthermore, basing on numerical simulation a universal energy-duration scaling relationship is suggested. The proposed Langevin equation provides a simple and physically reasonable picture by regarding the tectonic process as a process of Coulomb friction, where earthquakes are those transient (microscopic) stick-slip events during the process.

Keywords: Langevin equation, earthquake rupture, source process, slip distribution

Accelerating full-waveform inversion using source stacking followed by cross-correlation

Li-Wei Chen¹、Barbara Romanowicz²

(1)University of California at Berkeley, United States、(2)University of California at Berkeley, United States; Collège de France Paris, France; Institut de Physique du Globe, Paris, France

The spectral element method has been used for computing accurate synthetic seismic wavefields and has been successful at improving resolution in the full waveform global tomography. While its computational cost is still a challenging issue. Source stacking (Capdeville et al., 2005) has been proposed to effectively reduce the numerical cost in wavefield computations for global tomography. However high-amplitude fundamental mode surface wave always dominates the summed waveforms, where the contribution from overtone energy is hidden. With a misfit function defined by cross-correlating the summed waveforms between station-pairs, it is possible to boost the contribution of time windows containing overtones and body waves, as well as to apply a path-weighting scheme (Romanowicz et al., 2019). Since we can apply the same processing to the 3D synthetics and observations, and we have a good knowledge of location and mechanism, the quality of reconstruction of green's function is less important than in the case of Ambient Noise Tomography. To evaluate the capability of resolving the seismic structures, here we present a series of synthetic tests based on modified SEMUCB-WM1 (French and Romanowicz, 2015), in which a weakened radial anisotropy layer is replaced at the depth from range 30km to 50km. Also, we've collected a new real dataset and present our first application to the real data on a global scale.

Keywords: full-waveform global tomography

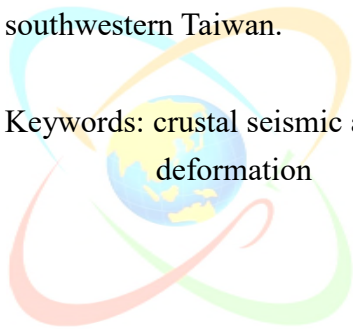
Revealing orogenic layered deformation by crustal seismic anisotropy in southwestern Taiwan

Cheng-Chien Peng¹、Ban-Yuan Kuo¹

(1)Institute of Earth Sciences, Academia Sinica, Taiwan

Taiwan orogenic belt results from the arc-continental collision of the Philippine Sea plate and the Eurasian plate. The complex collision deformation in the crust has been described by models with various depth extent. To examine those models, we investigate the crustal anisotropy in southwestern Taiwan and present a new shear wave splitting map that shows sophisticated yet systematic anisotropy patterns across the southwestern island. A notable feature is the delay time decrease from the coastal plain to the higher metamorphosed western foothills. Those observations could be modeled by the cooperation of the thickening orogeny-parallel anisotropy above the convergence-parallel mineral fabric at depths. Therefore, we prefer the layered deformation model that both the fold-and-thrust in the upper crust and the shearing in the lower crust control the crustal anisotropy manifested at the surface in southwestern Taiwan.

Keywords: crustal seismic anisotropy, southwestern Taiwan, orogeny, layered deformation



Earthquake Cluster analysis using Nearest Neighbor approach with unsupervised classifiers in Taiwan

Yu-Fang Hsu¹、Hsin-Hua Huang¹

(1)Institute of Earth Sciences, Academia Sinica, Taiwan

The spatiotemporal characteristics of earthquake clusters can shed light on the triggering process behind and physical properties of the crust. Taiwan is located at one of the most active orogenic belts with a high deformation rate and complex crustal structures and is expected to observe diverse earthquake activities, such as typical tectonic-driven mainshock-aftershock (M-A) sequences and fluid-driven swarms among different tectonic regions. Thus, a proper classification of earthquake clusters is critical for investigating the tectonic complexity and the varying triggering processes of local structures in Taiwan, which contributes to the seismicity hazard analysis. We produce the earthquake cluster catalogs with the combination of statistics-based nearest-neighbor approach (NNA) and density-based spatial clustering of applications with noise (DBSCAN) algorithm from January 1990 to June 2018 and further classify these earthquake clusters into M-A sequences and swarms with an modified k-means methods. In Taiwan, most of the M-A sequences are distributed around the major compression zones. The asperity sizes, time duration, and cluster events all show positive correlations with mainshock magnitudes in the M-A sequences. In contrast, the swarms are mainly distributed in the southern Central Range and the northern Hualien areas, which are spatially correlated with the high-fluid-flow regions. Also, the asperity sizes and cluster events show the low correlation with the mainshock magnitudes in the swarms.

Keywords: declustering, k-means, DBSCAN, classification, swarms

The influence of pore fluid pressure on earthquake b value in Southern California: a seismic velocity viewpoint

Sean Kuanhsiang Chen¹、Hsin-Hua Huang²、劉雅琪¹、Yih-Min Wu³、
Wei-An Chao⁴

(1)Department of Geosciences, National Taiwan University、(2)Institute of Earth Sciences, Academia Sinica, Taiwan、(3)Department of Geosciences, National Taiwan University; Institute of Earth Sciences, Academia Sinica, Taiwan; National Center for Research on Earthquake Engineering、(4)Department of Civil Engineering, National Chiao Tung University

Earthquake frequency-magnitude distribution in the crust commonly follows the b value from the empirical Gutenberg-Richter Power Law. Naturally, it is well-known that earthquake b value varies primarily with differential stress and earthquake faulting style and then varies with pore fluid pressure locally. So far, the influence of pore fluid pressure on b value can only be observed in the subsurface crust by injection wells. It remains unclear whether the effect is detectable in the scale of the entire crust. The seismic V_p/V_s ratio is sensitive to crustal crack density and pore fluid saturation to approximate pore fluid pressure in the crust. Southern California existed high-quality earthquake catalogs, velocity models, and similar earthquake faulting style, providing an ideal laboratory investigating how b value varies with V_p/V_s ratio. We find a positive correlation that the b value increases with V_p/V_s ratio in the Salton Trough region. This region with abundant earthquake swarms and creep events may imply high pore fluid pressure to vary the b values. This study highlights that V_p/V_s ratio can be used as an index to monitor b value variations for earthquake mitigation.

Keywords: earthquake b value, V_p/V_s ratio; pore fluid pressure, differential stress,
Southern California

New insights in seismic tomographic inversion to evaluate and validate Taiwan reference model

How-Wei Chen¹

(1)Department of Earth Sciences, National Central University

Over last three decays seismic tomography study in Taiwan is one of the principal geophysical techniques for illuminating 3D distribution of Earth structure across a range of scales. The usefulness of results is dependent on our ability to quantify its uncertainty. The uncertainty arises from the ill-posed nature of the tomographic inversion problem as multiple models are capable of satisfying the data. The assessment of uncertainty remains underdeveloped and is often ignored or given minimal treatment. The factors that control solution non-uniqueness include starting model, picking, ray or data coverage, data noise, parameterization, method used for data prediction and formulation of inverse problem. For those who make use of seismic tomography results may not have a full appreciation on their reliability through rigorously verification and validation. Tracing uncertainties can lead to significant improvement in the quantification of exploring structure imaging.

An effort to evaluate the uncertainty of available 3D models in Taiwan through travel-time calculations and wave propagation were performed. The uncertainty of using passive source data is relatively high compare to the use of active source data. Such result is directly linked to a key issue that without 2D data constraint, 3D inversion from 1D starting model produce considerable uncertainty. Shortest path or circular ray tracing is implemented for unstructured Delaunay triangulation mesh system. Ray tracing through tessellation triangle points for better path coverage can be achieved. The goal is to reduce the geophysical uncertainty when merge different types of data which carry various degree of errors while incorporate accurate geographic information into the model. Thus, mesh system preserves the actual suggestion of velocity distribution, geological boundaries, topography and bathymetry. Forward seismic ray tracing for such mesh system also shows better coverage, convergence and accuracy.

Keywords: uncertainty analysis, inverse problem, triangular mesh, triangular/circular ray tracing

Determination of platinum-group elements and Re–Os isotopes using ID-MC-ICP-MS and N-TIMS from a single digestion of geological samples

Kuo-Lung Wang¹、Zhuyin Chu²、Fu-Lung Lin³、Hao-Yang Lee³

(1)Institute of Earth Sciences, Academia Sinica, Taiwan; Department of Geosciences, National Taiwan University、(2)State Key Laboratory of Lithospheric Evolution, Institute of Geology and Geophysics, Chinese Academy of Sciences, Beijing, China、(3)Institute of Earth Sciences, Academia Sinica, Taiwan

A comprehensive method for the precise determination of Re and PGE (i.e., Os, Ir, Ru, Pt and Pd) concentrations as well as Re-Os isotopic compositions following Chu et al. (2015) is set up at IESAS in Taipei. About 2 g powder each sample were digested by the Carius tube method, and the Os was extracted by conventional CCl₄ method. The Re, Ir, Ru, Pt, and Pd were first subgroup separated from the matrix elements into Re-Ru, Ir-Pt, and Pd by a 2-ml anion exchange column. Subsequently, the Re-Ru was further purified by a secondary 0.25 ml anion exchange column to separate Re. The Pd and Ir-Pt were further successively purified by an Eichrom-LN column to completely remove Zr and Hf, respectively. Rhenium, Ir, Ru, Pt and Pd were individually measured by multi-collector inductively coupled plasma mass spectrometry (MC-ICP-MS) NuPlasma II, except for Os after microdistillation purification was analyzed by negative thermal ionization mass spectrometry (N-TIMS), Finnigan Triton TIMS, both instruments installed at IESAS. The measured Os isotopic ratios were corrected for mass fractionation using $^{192}\text{Os}/^{188}\text{Os} = 3.08271$ after interference corrections and oxygen corrections using $^{18}\text{O}/^{16}\text{O} = 0.002045$ and $^{17}\text{O}/^{16}\text{O} = 0.0003708$ (Creaser et al. 1991). The in-run precisions for Os isotopic measurements were better than 0.3% (2 RSD). During the analytical session in this study, the $^{187}\text{Os}/^{188}\text{Os}$ ratio of DROsS reference material was 0.1609 ± 1 (2 σ , n=25) on nanogram-sized loads measured with Faraday cups and 0.1607 ± 6 (2 σ , n=11) on 3.5–175 pg-sized loads measured with the electron multiplier; both agreed well with the previously reported value (0.16092; Luguet et al., 2008).

Keywords: Re–Os isotopes, platinum-group elements, ID-MC-ICP-MS, N-TIMS

Improvement of U-Th dating by refining uranium isotopic measuring techniques on MC-ICP-MS

Hsun-Ming Hu¹、Chuan-Chou Shen¹

(1)Department of Geosciences, National Taiwan University

Over the past decades, the development of speleothem U-Th (^{238}U - ^{234}U - ^{230}Th) dating techniques on multi-collector inductively coupled plasma mass spectrometry (MC-ICP-MS) has shed light for precisely reconstructing paleoenvironmental records back to 600 thousand years ago (ka). However, there are still two difficulties to build precise chronology for speleothem-based paleo-records with age >500 kyr. (1) For most 100s-kyr-old carbonates with only 100-200-ppb U, to determine precise ages is a challenge and a large sample size > 1-2 g is required. (2) Even for sample with high ppm-level U, it is difficult to apply U-Th dating to material with age older than 500 kyr, mostly hindered by the current analytical limitation of $\pm 0.2\text{-}0.4\%$ (2σ) on $^{234}\text{U}/^{238}\text{U}$. To measure precise $^{234}\text{U}/^{238}\text{U}$ ratio on a Thermo-Scientific Neptune MC-ICP-MS, we developed two new protocols with 2-sigma external errors of $\pm 0.7\%$ for 0.5 g carbonate with 100-200-ppb uranium and of $\pm 0.1\text{-}0.2\%$ for 0.5 g carbonate with 1-2-ppm uranium. Dynamic jumping modes with Faraday cups and a secondary electron multiplier were designed. The determined 2-sigma age errors are ± 1 kyr at 400 ka, ± 3 kyr at 500 ka, ± 5 kyr at 600 ka, ± 10 kyr at 700 ka and ± 20 kyr at 800 ka. The refined isotopic techniques offer the possible extension of speleothem-based proxy records to 800 ka.

Keywords: U-Th dating, U isotope measurement

In-situ LA-MC-ICPMS Si isotopic measurement for meteorites and terrestrial samples

Der-Chuen Lee¹、Yung-Hsin Liu¹、Hao-Yang Lee¹、Yu-Hsuan Liang¹

(1)Institute of Earth Sciences, Academia Sinica, Taiwan

In-situ laser ablation multiple-collector inductively-coupled-plasma mass spectrometry (LA-MC-ICPMS) for Si isotopic measurement has been set up at the Institute of Earth Sciences, Academia Sinica, in order to test the possibility of using Si isotopes to search for Ca-Al-rich inclusions (CAIs, the earliest condensates of the solar system) with fractionated unknown nuclear (FUN) isotopic effects. With identical petrographic and chemical compositions as the other CAIs, FUN CAIs exhibit ‰ to sub-‰ levels of this FUN isotopic effects, e.g., O, Mg, Si, Ca, Ti, and some other elements, which makes it extremely difficult to look for and to study the petrogenesis of FUN CAIs. We have previously set up *in-situ* LA-MC-ICPMS for Mg isotopes to search for FUN CAIs with good success, and thus decided to also set up *in-situ* LA-MC-ICPMS Si isotopes for the task. A 193 nm Analyte G2 excimer laser is coupled with a Nu-Plasma II, with a typical spot size of 50 micron and 50 sec integration time for each analysis, we are able to reproduce precise and accurate Si isotopic compositions of BHVO-2, while using the NIST612 as a standard. Preliminary *in-situ* LA-MC-ICPMS Si isotopic data for Allende CAIs are also consistent with the published results. Besides meteorites, with proper matrix-matching standards, this set up can also apply to terrestrial samples.

Keywords: LA-MC-ICPMS, Si isotope, CAI, meteorite, isotopic composition

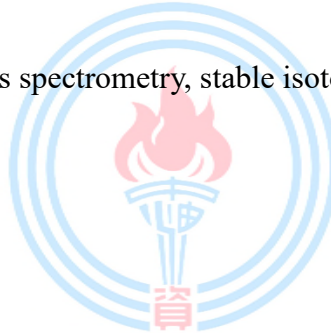
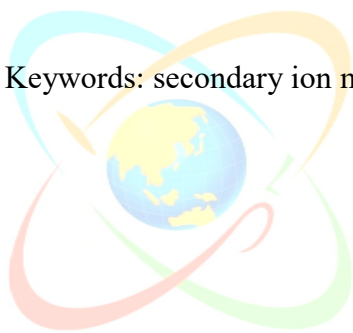
Reveal the devil in the detail: Nanometer-scale secondary ion mass spectrometry (Nano-SIMS)

Silver Sung-Yun Hsiao¹、Der-Chuen Lee²、Shang Hsien¹

(1)Institute of Astronomy and Astrophysics, Academia Sinica, Taiwan、(2)Institute of Earth Sciences,
Academia Sinica, Taiwan

Nanometer-scale secondary ion mass spectrometry (NanoSIMS) has been used for frontier researches in many fields including life, material, earth and planetary sciences. It can be used to study the spatial distributions of elements and stable isotope composition by very high spatial resolution (down to 50 nm per pixel) on the surface of solid samples. The only one NanoSIMS in Taiwan is setup in the core laboratory of interdisciplinary building of science and technology in Academia Sinica. It equips both cesium(Cs^+) and duoplasmatron oxygen(O^- or O_2^-) ion source that enable to analyze most metal and non-metal elements. And the trolley detectors (electron multicollector or faraday cup) can acquire signals of 7 specific isotopes simultaneously. Welcome to contact us for more collaborations.

Keywords: secondary ion mass spectrometry, stable isotope



國立臺灣師範大學地球科學系氬氬定年實驗室之分析儀器配置，

實驗步驟流程之簡介

葉孟宛¹、管賢志¹

(1)臺灣師範大學地球科學系

年代的探索與追尋一直是地質學非常獨樹一格的研究面向。 $^{40}\text{Ar}/^{39}\text{Ar}$ 定年法演伸自 K-Ar 定年法，是分析岩石礦物形成年代的方法之一。鉀元素廣泛存在於多種岩石與礦物之中，而氬氣則是惰性氣體，不易與其他化學物質反應，使得此兩種元素非常適合用來分析。固態鉀在經過中子照射之後，藉由同位素退變的關係，可轉化成氬，藉由高溫氣化或雷射燒熔的方式，將礦物與岩石中的氬氣釋放出來，進而量測岩石或礦物的「絕對年代」。國立臺灣師範大學地球科學系的氬氬定年實驗室承襲於過去國立臺灣大學地質學系的氬氬定年實驗室。共有三套質譜儀分別搭配可階段加溫式高溫爐、 CO_2 雷射與 193 nm 準分子雷射，並於 2017 年移交至師大。階段加溫定年系統：此系統以 VG1200S 質譜儀為分析主體，搭配雙真空，可升溫至 1600°C Mo 高溫爐與超真空樣本腔為採樣系統，採樣系統與質譜儀間則有一套超高真空不銹鋼全自動氣體純化系統。VG1200S 運用法拉第杯來偵測帶電粒子，通過測量 ^{40}Ar 、 ^{39}Ar 、 ^{38}Ar 、 ^{37}Ar 與 ^{36}Ar 的訊號而計算出樣本之年代。適用於年代老，變質或構造事件複雜之礦物與岩石。雷射燒熔定年系統：此系統以 VG3600 質譜儀為分析主體，搭配新銳 CO_2 (二氧化碳)雷射並配合超真空樣本腔為採樣系統—可以連續或脈衝形式使用於單顆粒標本燒結定年及階段加溫分析之用。VG3600 運用法拉第杯與倍增管來偵測帶電粒子，由於倍增管的偵測靈敏度為法拉第杯的 100 倍，因此本分析系統適用於地質事件單一，年代年輕，樣本量小，但可能需要大量數量分析之礦物與岩石。雷射探針定年系統：此系統以 Nu Noblesse 質譜儀為主體，利用專利的聚焦設備進行同位素的多重接收，並配合 UP193-FX 準分子雷射與超真空樣本腔為採樣系統，可進行定點微區定年及單礦物燒熔定年實驗分析。此技術提供了一個直接量測礦物內氬同位素分布最方便直接的方法，進而可以求得礦物內的年代剖面。可進行構造、變質岩溫壓及年代之直接比對與連結。本實驗室所分析之礦物與全岩樣本之純化皆於師大地科之礦物分離實驗室進行，而後序之中子照射於清華大學水池式反應器 (THOR) 進行。並以 Fish Canyon Sanidine (28 Ma) 及 MMhb-1 (519.8 Ma) 為標準礦物與樣本共同照射。質譜儀之大氣校正值則依據 Lee 等人 (2006) 所提出的 $^{40}\text{Ar}/^{36}\text{Ar}=298.5$ 。儀器控制軟體則有美國地質調查所所發展之 Ar AUTO 與台大原來之控制系統並行。數據分析與圖表輸出軟體則為美國地質調查所所發展之 ARAR*與 ISOPLOT。

中文關鍵字：氬 39 -氬 40 定年法、分析儀器、分析步驟

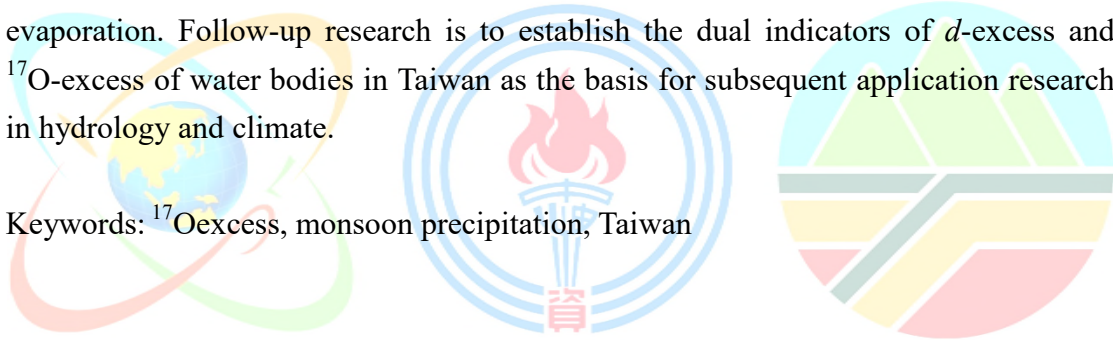
Triple oxygen isotope compositions of Taiwan precipitation

Tsung-Ren Peng¹、Wen-Jun Zhan¹

(1)Department of Soil and Environmental Sciences, National Chung Hsing University

In this report the results of the triple oxygen isotope compositions, including $\delta^{17}\text{O}$, $\delta^{18}\text{O}$, and ^{17}O excess defined by $\ln(\delta^{17}\text{O}+1) - 0.528 \times \ln(\delta^{18}\text{O}+1)$, of Taiwanese monsoon precipitation are presented. The samples are collected in Daliao (S. Taiwan), Yi-Lan (N. Taiwan), and Wuling (C. Taiwan), respectively, and are analyzed using Picarro L2140-i isotopic water analyzer (IWA). The analytical precisions of the IWA expressed as 1s for the laboratory standards are better than 0.018‰ for $\delta^{17}\text{O}$ and 0.028‰ for $\delta^{18}\text{O}$, respectively. Some critical hydro-climatological implications of $^{17}\text{O}_{\text{excess}}$ regarding Taiwan are briefly listed below: (1) Humidity conditions in the air mass source areas of summer and winter precipitation are similar. (2) Both summer and winter precipitating vapors are almost formed under isotopic equilibrium, but winter precipitating vapor encounter additional kinetic fractionation. (3) Most precipitations are significantly affected by secondary evaporation. Follow-up research is to establish the dual indicators of d -excess and ^{17}O -excess of water bodies in Taiwan as the basis for subsequent application research in hydrology and climate.

Keywords: $^{17}\text{O}_{\text{excess}}$, monsoon precipitation, Taiwan



利用原位動態拉曼串聯在線式質譜儀觀察含銅/二氧化鈦與一氧化碳

反應之結構變化

楊汶達¹、劉雅瑄¹

(1)臺灣大學地質科學系

礦物的晶相會隨受到外界的溫度與壓力的影響，進而產生所謂的晶相轉變，可是礦物在自然環境中的晶相轉變則遠比我們所認知的更為複雜，尤其當有水氣介入或是在不同的氣體組成條件下，其變化的行為仍猶未可知。

在本研究中，我們利用質子流量控制器協助模擬煙道環境，並通入裝有含銅之二氧化鈦粉(Cu/TiO_2)末之反應器中(heating stage (Linkam))，利用原位動態拉曼光譜儀(Operando Raman)觀察 Cu/TiO_2 材料隨著反應溫度上升與一氧化碳(CO)的催化行為模式，並將反應後之氣體利用在線式質譜儀觀察其變化情形，以利協助釐清反應過程中材料與反應氣體間的交互作用，此舉不僅可以建構可能的反應途徑與機制，更可以用於提升材料的反應性。

實驗結果顯示 CO 藉由 Cu/TiO_2 催化氧化為二氧化碳，此過程中 TiO_2 的結構隨溫度變化有明顯的拉伸情形，但並未改變其晶相，是由於反應過程中 TiO_2 出現氧空缺，並由環境中的氧來補給。本研究藉由原位動態拉曼光譜有效的觀察到材料與反應過程之相關性，並有助於發展一氧化碳低溫去除裝置。

中文關鍵字：原位動態拉曼、在線式質譜儀

一件三角龍屬新頭骨標本的形態描述與初步分類

蕭語富¹、蕭琮諭²、劉振軒³、廖俊棋⁴、周冠宇⁵、黃威翔³、楊子睿⁶

(1)中國文化大學地質學系、化石先生股份有限公司、(2)臺北市立大學地球環境暨生物資源學系、
(3)臺灣大學獸醫學系、(4)中國科學院古脊椎與古人類研究所、(5)中興大學生命科學系、(6)國立
自然科學博物館、成功大學地球科學系

自 19 世紀末的化石大戰（Bone Wars）開始，E.D. Cope 與 O.C. Marsh 兩人命名了上百種的恐龍。其中，最有名的恐龍就是在侏儸紀公園系列便風光亮相的三角龍屬（*Triceratops*），而且絕大多數的三角龍屬化石都出土於美國。然而，現今多數標本仍有保存不佳與部分缺失的問題。本研究描述一件挖掘自美國蒙大拿州地獄溪層（Hell Creek Formation）的三角龍屬新頭骨標本，並參考 Forster 於 1996 年根據數件三角龍屬標本所得到的形態統整，討論此新頭骨標本的分類地位。根據其頭骨縫合線、眶前角與鼻角的形態等差異，顯示本研究之頭骨標本同時具有 *T. horridus* 與 *T. prorsus* 之特徵，可能為新的三角龍屬物種，然而確立新種尚需進一步的分類學研究。此外，此新頭骨標本上有一些撞擊、爪痕等疑似受傷後癒合的記錄，透過未來的病理組織學與爪痕對比，此新頭骨標本可幫助古生物學家進一步瞭解三角龍屬過去與其它物種的交互作用與其生活型態。

中文關鍵字：病理組織學、侏儸紀公園、蒙大拿州、地獄溪層、爪痕



以魚耳石討論臺灣更新世以來大黃魚(*Larimichthys crocea*)成長速率

與年齡結構之變化

王彥鈞¹、林千翔¹、蕭仁傑²、鍾銘宗³、李匡悌⁴、飯塚義之⁵、
張至維⁶

(1)中央研究院生物多樣性研究中心、(2)臺灣大學海洋研究所、(3)東京大學大氣與海洋研究所、
(4)中央研究院歷史語言研究所、(5)中央研究院地球科學研究所、(6)國家海洋研究院

漁業活動所造成的海洋生態衝擊已明顯改變了魚類群聚構造以及不同物種內的生活史策略，但如何將之量化並評估其影響範圍仍是現今海洋保育、生態管理上重要的挑戰。硬骨魚類的耳石由於能夠長期保存在地層中，其外部形態不僅能作為分類依據，亦可藉由定齡技術重建其生活史特徵，因此耳石是分析魚類在長時間尺度下受環境變遷壓力所產生生活史變化極有潛力的研究材料。本研究首先重建更新世之古魚類群聚構造，並針對數量豐富，但目前卻因漁業壓力導致野外瀕危之大黃魚(*Larimichthys crocea*)，由化石露頭、臺南科學園區新石器時代早期至鐵器時代考古遺址與現生族群耳石年齡成長及穩定性碳氧同位素分析，探討其族群結構及生活史自更新世以來，隨人類漁業壓力增加，如何出現生活史策略上年齡成長的改變。初步結果指出大黃魚的成長與過去有顯著差異的現象，推斷與漁業壓力逐漸增加有關。

中文關鍵字：嘉義牛埔、台南科學園區遺址、古生物學、碳氧同位素分析、魚類硬組織定齡學

墾丁石灰岩洞穴內鼠類化石之研究

張鈞翔¹、王國全²

(1)國立自然科學博物館、(2)成功大學地球科學系

墾丁森林遊樂區一處石灰岩洞穴中發現大量陸相哺乳動物化石，該化石群落埋藏了以骨質為主的本體化石，未受明顯之風化作用，亦無被礦物置換或取代。本研究針對具有特定環境選擇偏好且數量眾多、繁衍速度快的小型啮齒動物，透過臼齒形態特徵建立形態模型，並與現生種比對其中之差異。可用於比對之現生種，一為在臺灣一屬一種的高山田鼠 (*Microtus kikuchii*) 目前棲息於海拔兩千公尺以上的高山，其生理條件不適合生存於熱帶氣候，受限於高山島嶼之上，喜愛草原棲地。另一白腹鼠屬現有兩種，分別為分布於低海拔的刺鼠 (*Niviventer coninga*) 與高海拔的高山白腹鼠 (*Niviventer culturatus*)，皆為森林型物種，但刺鼠可以適應森林邊緣過渡至草原的環境。化石標本經過形態描述對比以及量測數據統計判斷較接近高山田鼠與刺鼠，上述兩種化石之發現，推測臺灣南部更新世晚期之環境以草原為主，高山田鼠在當時尚存於恆春地區，直到氣候變遷，競爭失利的牠們才播遷至高山地區。

中文關鍵字：形態學、墾丁、石灰岩洞穴、啮齒目、化石



Fossil scleractinian community in Taiwan

Lauriane Ribas-Deulofeu¹、Chien Hsiang Lin¹

(1)Biodiversity Research Center, Academia Sinica, Taiwan

Taiwanese reefs are among the most diverse marine ecosystems on earth, hosting 558 scleractinian species and over 1400 reef fish species. However, the multiple anthropogenic pressures along with the highly active typhoon regime and recurrent heat stress anomalies have induced major local degradations of the reefs. While modern Taiwanese reef biota have been relatively well characterized, little is known on their past long-term evolutionary trajectory which led to the diversification of this particularly highly diverse scleractinian coral communities. Furthermore, there is an important scarcity in research investigating functional aspects of Taiwan's fossil reefs. Individual coral fossils from diverse locations in the island have been reported since the 1940s. However, specimens and reports are scatter in diverse organizations and nearly all of them are not available online. We aim to inventory the existing information on fossil corals and, further identify potential spatial and temporal knowledge gaps to reconstruct, at geological scale, the development of the scleractinian coral communities in Taiwan. Here, using our recent find on late Miocene *Dendrophyllia* specimens in northern Taiwan as an example, we demonstrate the fact that fossil corals are highly underrepresented to the regional paleontological community. In addition, our project aims to investigate past functioning of coral reef ecosystems in Taiwan by extending the specimen descriptions to the other taxonomic groups associated with fossil corals. Ultimately, with this knowledge, we will be able to better predict coral reef's survival capacities under the ongoing climate change and anthropogenic pressures.

Keywords: paleo-ecology, coral reef, fossil scleractinian diversity, Taiwan

Investigation of the stiffness of dinosaur eggs and the feasibility in contact-incubation in the aspect of mechanics

Hsiao-Jou Wu¹、Hon-Tsen Yu¹、Jia-Yang Juang²

(1)Department of Life Science, National Taiwan University、(2)Department of Mechanical Engineering,
National Taiwan University

Extant avian egg may be regarded as a naturally perfect design. It has to be fragile enough to let the chick out, meanwhile, it has to be stiff enough to bear the load induced by its parents during contact incubation. In our previous work, we studied the eggshells of over 1000 avian species, and defined a dimensionless number C (also called C number) to quantify the shell stiffness across a wide range of egg size. We found that C number was largely constant among Aves. The lowest limit of contact-incubation was also defined in the aforementioned study. In this paper, we applied the same method to fossil dinosaur eggs to analyze if contact incubation is possible for these dinosaurs. Our finite element analysis allows us to create egg models in the computer and simulates how the eggs deform and break under the contact-incubation scenario. We focus on the clutch specimens with relatively better preservation (such as troodontid and oviraptorosaurian clutches). Our study may shed new light on the incubation behavior of non-avian dinosaurs and the evolution of contact incubation of amniote eggs.

Keywords: dinosaur egg, eggshell, dimensionless number, contact-incubation

Late Miocene otoliths from northern Taiwan: insights into the rarely known Neogene coastal fish community of the subtropical northwest Pacific

Chien-Hsiang Lin¹、Chi-Wei Chien²

(1)Biodiversity Research Center, Academia Sinica, Taiwan、(2)Department of Petroleum Geology,
Exploration & Development Research Institute

Knowledge of Neogene fish diversity in Taiwan is extremely limited. In this paper, we present a collection of 1716 fish otoliths recovered from the late Miocene lower-most Kueichulin Formation along the Dahan River in Shulin, New Taipei City; the collection provides insights into the past fish fauna of the subtropical northwest Pacific. The abundance and density of otoliths vary across the sites. Although the preservation of samples is considerably limited, our sample coverage is sufficient and reveals the presence of at least 34 otolith-based taxa belonging to 13 families. Four new species are introduced: *Larimichthys koeae* sp. nov., *Nibea chaoi* sp. nov., *Taosciaena jiangi* sp. nov., and *T. hui* sp. nov. The assemblage is dominated by otoliths of Sciaenidae, Gobiidae, and Soleidae. Among the earliest fossil records, this collection features a remarkable abundance of *Larimichthys* spp. All otolith samples are indicative of a coastal shallow-water palaeoenvironment with muddy to sandy bottoms. Furthermore, the fish assemblages were perhaps adjacent to a river mouth. We hypothesize that the differences in the taxonomic composition between the Shulin assemblage and modern fauna are mainly chronological and evolutionary, and a mild turnover of certain lineages has occurred since the Miocene.

Keywords: Kueichulin Formation, palaeodiversity, taxonomy, *Larimichthys*,
Sciaenidae, palaeoecology

臺灣南部晚更新世金鯛(鯛形目鯛科)之化石紀錄

歐鑫岳¹、林佳燕²、陳鴻鳴³、林千翔²

(1)東海大學生命科學系、(2)中央研究院生物多樣性研究中心、(3)臺灣海洋大學水產養殖學系

本研究針對恆春地區晚更新世發現之鯛魚結核化石進行形態描述與分類鑑定。化石樣本採集於恆春鎮頭溝里的溪溝中，層位屬於四溝層，由富含陸源矽質碎屑的泥質砂岩與海洋生物碎屑岩所組成，年代約在 9-14 萬年前。四溝層沉積環境屬於潟湖至河口灣，水深約在 0 至 20 公尺間。此件鯛魚結核化石長約 21 公分，寬約 11.5 公分；魚體長約 15.8 公分，寬約 8.2 公分，出露面為原始風化面，出露骨骼多位於魚體左側，上下顎牙齒形態清楚，有利於後續鑑種辨識。本次研究透過牙齒形態學與臺灣現生所有鯛科魚類比較分析，發現其與現生鯛形目鯛科的金鯛(*Chrysophrys auratus*)相同，為臺灣首次化石記錄。此標本目前典藏於中央研究院生物多樣性博物館，館藏編號為：ASIZF0100141。

中文關鍵字：齒列、牙齒形態、魚化石、結核、化石紀錄分析、金鯛



非彈性應變回復法現地應力評估的統計分析與精進

蔡維倫¹、陳炳權²、楊士寬¹、葉恩肇¹、林立虹³、柯建仲⁴

(1)臺灣師範大學地球科學系、(2)臺灣中油公司、(3)臺灣大學地球科學系、(4)中興工程顧問社

隨著科技水平不斷進步，為提升生活品質，人們對於交通網路建設、天然資源開採、廢棄物處置與空間開發及擴建等需求與日俱增。在這些工程發展的促使下，現地應力在工程及研究上相當重要的參數。現地應力不僅影響開發中結構物的穩定性，對於地下岩盤壓力、水文環境及對不同深淺層岩盤的開挖破壞行為強度控制有著相當關聯性，因此，近年來現地應力狀態的研究日趨重要及重視。現地應力測量有多種不同方法，如套鑽法、水力破裂和非彈性應變回復法等，其中又以非彈性應變回復法(Anelastic Strain Recovery, ASR)為目前的耗費成本較低、效率較高的現地應力測量方法(孫東生等人，2014)。ASR 法是利用地下深處岩石因應力解壓後所產生的應變回復來推算三維現地應力方向和規模的方法。

前人使用的非彈性應變回復分析程式是以 18 個應變計測量 9 個方向的回復正應變規模，重建三維應變張量，進行三維主應變場的演算，轉換成主應力方向與規模，但結果只獲得一組平均數值，並未分析各方向與規模的偏差量，以致無法提出可信的數據供工程單位參考使用。本研究預計進行原程式的改進，將原本 9 個方向改以 6 個獨立方向為一組單位，並於每個獨立方向使用 4 個應變計進行量測，運用抽樣的方式進行重複演算，將比對每一組結果之應力方向與規模的異同，完整地獲得統計意義與誤差範圍的結果。

統計分析方法之樣本取於臺東南橫大崙溪，深度 140 米之片岩樣本。ASR 初步初步分析結果顯示為非典型安德森斷層應力場形式。最大、次大和最小主應變之位態分別為 $141.14^{\circ}/45.79^{\circ}\text{E}$ 、 $36.22^{\circ}/14.05^{\circ}\text{E}$ 和 $293.74^{\circ}/40.81^{\circ}\text{W}$ ，水平最大應力的擠壓方向為西北-東南向，主應力由大到小分別為 3.66、2.22 和 2.06 MPa。葉理傾向和傾角分別為 296.18° 和 65.31° ，葉理面的法向量與三軸主應變相距較遠，推測本樣本可能沒受到葉理面力學異相性的影響。未來工作將會進行抽樣與統計分析，將這些新資料運用新的改良方式進行演算，得到較高可信度的應力場大小。冀望未來此新技術可以廣泛運用於各項工程開發與地質科學學術研究。

中文關鍵字：非彈性應變回復法、現地應力場

台灣瑞穗地區地熱探勘的初步進展與挑戰

林義凱¹、殷瑤萱¹、洪煒晴¹

(1)倍速羅得股份有限公司

學術單位的研究報告指出，地熱資源在台灣非常豐富，且極具開發潛力。由於國內地熱蘊藏具開發之潛力且與地熱資源開發利用相關之法規、技術、環境等方面之發展日漸成熟，另能源白皮書預定在 2025 年時要達到地熱發電裝置容量 200MWe 之目標，倍速羅得股份有限公司(以下簡稱本公司)將配合政策積極開發國內地熱資源，期能以團隊之經驗、能力與專長合作投入地熱發電產業之發展。目前本公司於花蓮瑞穗地區已完成初步地質調查，並選定一合適場址進行鑽探調查。由於台灣東部地區之地熱模式主要係由地質構造所控制，因此針對斷層及裂隙的掌握是本區域開發的關鍵。於花蓮瑞穗地區，地層主要為玉里層，岩性主要屬黑色至灰色片岩偶夾石英岩脈。於本案基地有加星斷層通過，基地位於斷層破碎帶上，為地下之熱液提供良好的通道。

中文關鍵字：地熱、裂隙、斷層



大屯山地熱區之三維地電阻模型及其含義

董倫道¹、郭泰融¹、林蔚¹、林朝彥¹、陳棋炫²、張育仁²、林昶成²、曾振章¹、張祐銓¹

(1)工業技術研究院材料與化工研究所、(2)經濟部中央地質調查所

為瞭解大屯山地區的地熱地質構造，本研究於 2020 年進行了寬頻大地電磁探測，探測範圍擴大涵蓋西北側山腳斷層及東南崁腳斷層，以便能獲取較完整的地熱構造空間資訊。本研究採取階段逆推程序及 nested modeling 技巧，獲得水平網格為 250 m 的三維地電阻模型，與空中磁測、地表線型、微震震源分布及既有鑽井礦物分布等資訊對比良好，故能作為後續建構地熱構造之基礎。由國際間類似地質區的大地電磁探測經驗及本區既有鑽井資訊，顯示大屯火山區下伏的沉積岩基盤內有侵入火成岩體存在，具有中和酸性熱液的功能。而安山岩體內電阻率接近 1 ohm-m 的區域可對應受偏中性熱水換質後富集的蒙脫石，是安山岩地熱田重要的指標黏土蓋層。依據三維地電阻模型，本研究共篩選出 8 處潛在地熱區，但若考量未來開發難易與國內地熱開發時程，則可進一步篩選出 5 處場址，可作為後續進一步精查的對象。

中文關鍵字：大屯山、地熱、大地電磁、三維地電阻模型、地熱構造



大屯火山群小油坑區域之無人機高解析度熱影像成果

江晉霆¹、詹瑜璋¹、孫正璋²、張國楨³

(1)中央研究院地球科學研究所、(2)中央研究院地球科學研究所、臺灣大學地質科學系、

(3)臺北科技大學土木工程系

傳統熱影像儀多半用於軍事、防災、醫學及工程等用途；拜科技日益新穎所賜，熱影像儀已縮小至無人機可乘載之重量且解析度日趨精細，因此可以將熱影像儀結合無人機進行拍攝任務，再將獲取之熱影像進行建模分析，而我們所使用之熱影像儀也有結合可見光相機，執行任務時可同時獲取可見光影像與熱影像，在天氣狀況不同時，兩種影像可以互補。本研究探討無人機結合熱影像儀後，所生成之熱影像模型之用途。本研究使用無人機掛載熱影像儀進行拍攝。現場執行任務前要先布置航空標以利日後模型建置，但此處航空標與一般可見光影像的航空標有所不同，需在航空標上貼上鋁箔，因為鋁箔的放射率較低，才能在熱影像上明顯看到航空標位置。而熱影像儀的解析度較低，因此航線規劃上，相對於一般可見光影像需要較高的重疊率。任務完成後再回到室內使用軟體生成熱影像模型。本研究區域為陽明山國家公園的小油坑，小油坑位於七星山西北麓，海拔約 805 公尺，此研究區域因後火山作用，有許多的噴氣孔形成，這些噴氣孔終年有硫氣與蒸氣噴出且維持一定的溫度，因此選擇小油坑作為無人機與熱影像測試區塊。本研究使用高解析度熱影像儀搭配無人機近距離拍攝可產製出高解析度熱影像模型，從熱影像模型中可以得知噴氣孔的溫度，未來可由熱通量計算進而估略出該區塊之地熱能，期許此方法有助於未來能源開採的前期作業。

中文關鍵字：無人機、熱影像、小油坑區域

大屯山硫磺子坪地熱發電示範區地熱潛能調查分析

楊智豪¹、雷世璋¹、俞旗文¹、陳思溥²、雷修懿²、林伯耕²、林伯修²

(1)中興工程顧問社、(2)結元能源開發股份有限公司

根據以往學研單位估計全台地熱潛能區的調查相關研究顯示，大屯火山地區地熱潛能高達 514 MW。政府再生能源的既定政策目前設定 2025 年，達成地熱發電累積設置 200MWe 的目標。爰此，能源局在 2018 年積極推動新北市硫磺子坪地熱發電示範區計畫案招商，此示範案由結元能源開發股份有限公司(結元公司)奉核執行，示範場址位於陽明山國家公園東北側的硫磺子坪地區(LHZIP site)，大致於磺嘴火山錐北側靠近天籟溫泉區。結元公司於 2019 年起啟動硫磺子坪地熱發電示範區內一系列場址調查研究(簡稱探勘階段)，項目包含地電阻率影像剖面調查(RIP)、兩口淺部調查井鑽探(S1 井 80 米，L1 井 200 米)、岩屑取樣分析、地熱流體取樣分析等，並同時委託日本 GERD 公司於場址周邊地區進行大地電磁(MT)分析調查，分析範圍長寬各約 4 公里。

本文概述本案探勘階段，調查試驗與 MT 分析成果的綜合研判。兩口淺部調查井鑽探岩屑分析結果顯示：四磺子坪地區的 S1 井淺部安山岩已受到強烈的熱水換質作用；硫磺子坪地區的 L1 井，較淺部局部裂隙發達處有明顯熱水換質作用，且熱水換質區段 pH 值相當低。根據 RIP 影像剖面、調查井水位，比較位於北側鄰近能源局委託工研院 2014 年所鑽地熱井(E303)的地質剖面與地下水面差異推測，硫磺子坪場址東側邊緣有一水文邊界。此外，從 MT 分析結果可推測海拔 300 公尺處，四磺子坪至硫磺子坪有一西北-東南走向的呈帶狀分布的低阻帶，初判為熱儲層之蓋岩(Cap rock)；海拔 100 公尺處，L1 井西北方有一高阻帶，推測可能為乾蒸氣聚集的區段。綜合各項資料推估，探勘地區熱源可能來自磺嘴山底下的岩漿庫。本文利用大地電磁試驗結果，以 USGS 體積評估法估算目標區(4x4 平方公里)熱儲層的總熱能，再以有效回收熱能轉換電能來評估發電潛能約為 24.38 MWe。

中文關鍵字：地熱發電、硫磺子坪、地電阻率影像剖面(RIP)、大地電磁(MT)

陽明山國家公園地區地熱開發可行性規劃

王祈¹、宋聖榮¹、盧乙嘉¹

(1)臺灣大學地質科學系

台灣地區位於歐亞板塊與菲律賓海板塊相互碰撞的板塊邊緣，處於環太平洋島弧帶，火山與地震活動頻繁。主要的火山分布於北部的大屯火山群，有明顯的火山地形與地表地熱徵兆，加上特有的地理條件，成為陽明山國家公園內獨特的地質地形景觀。經由前人以各類探勘方法的評估研究，台灣北部大屯火山地區的地熱潛能可達 500 MWe 以上。依循政府能源發展綱領，為達成 2025 再生能源發電占比達 20% 的政策，近年經濟部能源局已在大屯火山區的陽明山國家公園外圍，協同地方政府選擇適當的地熱潛能區，進行地熱發電示範廠區及其他地熱利用計畫的開發。有鑑於大屯火山區地熱潛能範圍仍有廣大區域分布在國家公園境內，為兼顧經濟發展與環境永續，順利推動綠色能源轉型，達成國家再生能源發展目標，可以思考並參照其他國家的做法，或許有條件的鬆綁陽明山國家公園內某些土地分區的天然資源開發使用規範，亦可進一步的由鑽探研究來了解並監測火山活動及環境指標，在最不影響生態環境的前提下達成多贏的共識。我們針對在最低限度開放國家公園土地使用的前提下，預先分析地熱開發的可行性評估，套用有利探勘標的分析法則，將地底地質條件，人文環境保育規範，自然災害敏感度作為分析因子，製作數位圖層類別，使用前人的地熱潛能分布，加上陽明山國家公園的各級土地分區，以及過去的陽明山國家公園的地質災害敏感區分級調查及山崩地滑地質敏感區研究報告，以疊圖方式來檢視在陽明山國家公園內的潛在地熱探勘地點，待相關法令鬆綁，即可著手進行國家公園內的地熱探勘，利用天然地熱資源，亦可監測與研究火山相關活動，防患於未然。

中文關鍵字：地熱探勘、國家公園、人文法規、大屯火山群、有利探勘標的法

對 1997 林肯大郡順向坡滑動與其結構物災損的新見解

李忠勳¹、林承翰¹、柳鈞元²、方儒雅¹、林銘郎¹

(1)臺灣大學土木工程學系、(2)中興工程顧問社

1997 年 8 月 18 日汐止林肯大郡社區北側順向坡在溫妮颱風期間發生滑動，滑動塊體直接衝擊下邊坡五樓建築群，同時造成 28 名人員罹難。過去針對本處順向坡滑動之肇因與機制雖已有諸多調查研究報告，然而對於順向坡滑動引致結構物損壞的行為，因缺乏有效的分析工具仍未有深入探討；另外，林肯大郡事件後在相同地質區中仍有嚴重順向坡災害發生，且近年利用高精度地形資料在研究範圍內圈繪出許多順向坡地形。因此本研究回顧歷史航空影像、災害前後地形測繪資料、災後調查報告與勘災影像，重新定位林肯大郡事件中順向坡滑動與結構群破壞之空間位置，並透過不同比例尺地質圖、LiDAR 陰影圖與補充地表地質調查，釐清區域尺度之地層岩性分布與場址尺度中節理線型之關係，進而建立三維地質模式。最後本研究利用離散元素分析方法允許元素分離、斷裂與位移之優勢，建立模擬順向坡與結構物互制行為之三維力學模型。模擬成果顯示災害過程中順向坡塊體將裂解形成二次滑動，且結構物因空間分布與配置方式將有不同程度的損害。未來將運用此數值模型量化分析順向坡滑動與衝擊結構物之動態過程，以提供針對順向坡破壞引致結構物損害之評估參考。

中文關鍵字：岩石邊坡、林肯大郡順向坡滑動、山崩與結構物互制、離散元素法分析、三維地質力學模型

多平面分析法於三維邊坡穩定性分析之研究-以霧鹿場址為例

黃淳銘¹、鍾明劍¹、陳建新¹、趙韋安²、戴東霖³

(1)中興工程顧問社、(2)陽明交通大學土木工程學系、(3)經濟部中央地質調查所

本文以台東縣霧鹿場址為例，採用 SoilVision 軟體中的 Multi-Plane Analysis (簡稱 MPA) 分析方法，透過極限平衡法進行多平面分析，用以探討區域尺度之邊坡穩定性。霧鹿場址的分析模型係利用研究區域內的鑽探及地物探勘資料，建出 AA' 及 BB' 剖面，並將此區域材料劃切為五層，分別為土壤層、舊崩積層、階地堆積層、剪裂帶、黑色片岩，再以內插方式，將二維剖面分層往第三維度方向延伸，以建立出分析所使用的三維模型。本文除依照觀測水位資料，設定常時水位、高水位兩種分析情境外，並於常時水位加入地震力作用影響，作為第三種分析情境，藉此根據霧鹿場址於上述三種分析情境下之安全係數分布情況，進而探討霧鹿場址之安定性與易致災山崩熱區。

由三維模擬分析結果，得以初步評估霧鹿場址邊坡安全係數分布情況，因觀測期間水位變化不大，故常時水位及高水位情境差異較不明顯，分析成果皆顯示場址大致上處於穩定情況。但地震力的加入，使邊坡安全係數值大幅下降，於階地堆積層及舊崩積層區域穩定性相對較低，需多加留意。整體而言，透過 MPA 技術進行邊坡穩定性分析，能夠有效且快速瞭解邊坡的安全係數三維等值圖，讓研究者能視覺化感受研究區域內的安全係數分布狀態、易崩塌區域、塊體大小及運動方向，有利於研判易致災山崩熱區，並進行後續防減災對策之研擬。

中文關鍵字：大規模崩塌、情境模擬、多平面分析法、霧鹿場址

The analysis of the 2020 Hpakant Jade Mine slope failure event using multi-sensor data integration

Yunung Nina Lin¹、Edward Park²、Yu Wang³、Yu-Pin Quek²、Jana Lim²、Enner Alcantara⁴、Huuloc Ho⁵

(1)Institute of Earth Sciences, Academia Sinica, Taiwan、(2)National Institute of Education, Nanyang Technological University, Singapore、(3)Department of Geosciences, National Taiwan University、
(4)Department of Environmental Engineering, Sao Paulo State University, Brazil、(5)Water Engineering and Management, Asian Institute of Technology, Thailand

Northern Myanmar is currently the largest jade mining area around the world, with most of the mining activities occurring near the Hpakant area. The rapid expansion of jade mining in the past decade has significantly modified the topography, and triggered frequent fatal landslides in the mining quarries. The landslide in the Wai Khar open-pit jade mine on 2 July 2020 is one of the recent examples of quarry failure in the region, killing at least 172 jade miners in one single failure event. In order to understand the landscape evolution and the potential causes of this landslide, we integrate remote sensing observations from both optical satellite images and Sentinel-1 InSAR time-series, together with multi-temporal digital elevation models (SRTM and AW3D30), Landsat-based soil moisture time-series, CHIRPS precipitation time-series, and the video footages of the mining site before and after the landslide, to investigate the change of the Wai Khar open-pit mine between 2000 and 2020. Our result points out that the Wai Khar mining site is under aggressive mining cycles exacerbated by frequent, uncontrolled landslides. The tailings, which many have been turned into the residential areas north of the quarry pit, shows rapid subsidence especially near the rim of the pit. Rapid compaction of the tailings likely causes water expulsion and induces seepage failure. Since the precipitation record suggests below-average rainfall in the beginning of the 2020 monsoon season, the occurrence of landslide means the sliding planes were already in critical state. This critical state is manifested by the accelerated subsidence around the collapse area since the beginning of 2020. Altogether, our study suggests the Wai Khar open-pit failure is not directly caused by extreme rainfall, but by the combinations of weak geology and improper planning/management of the mining site.

Keywords: open-pit mine, slope failure, seepage failure, tailing subsidence, InSAR time-series, phase linking

Developing modified Bi-viscosity model for studying the mudslide fluid dynamics

Tso-Ren Wu¹、Thi-Hong-Nhi Vuong¹、Chun-Wei Lin¹、Chun-Yu Wang²、
Chia-Ren Chu²

(1)Graduate Institute of Hydrological and Oceanic Sciences, National Central University、

(2)Department of Civil Engineering, National Central University

This paper incorporates Bingham and bi-viscosity rheology models with the Navier–Stokes solver to simulate the dynamics and kinematics processes of slumps for tsunami generation. The rheology models are integrated into a computational fluid dynamics code, Splash3D, to solve the incompressible Navier–Stokes equations with volume of fluid surface tracking algorithm. The change between un-yield and yield phases of the slide material is controlled by the yield stress and yield strain rate in Bingham and bi-viscosity models, respectively. The integrated model is carefully validated by the theoretical results and laboratory data with good agreements. This validated model is then used to simulate the benchmark problem of the failure of the gypsum tailings dam in East Texas in 1966. The accuracy of predicted flood distances simulated by both models is about 73% of the observation data. To improve the prediction, a fixed large viscosity is introduced to describe the un-yield behavior of tailings material. The yield strain rate is obtained by comparing the simulated inundation boundary to the field data. This modified bi-viscosity model improves not only the accuracy of the spreading distance to about 97% but also the accuracy of the spreading width. The un-yield region in the modified bi-viscosity model is sturdier than that described in the Bingham model. However, once the tailing material yields, the material returns to the Bingham property. This model can be used to simulate landslide tsunamis.

Keywords: mudslide, Bingham, bi-viscus model, rheology, landslide tsunami, local scour

大規模崩塌的場址調查－以宜蘭縣大同鄉 D007 梵梵場址為例

康耿豪¹、陳建新²、鍾明劍²、趙韋安³、魏殷哲⁴、劉興昌⁴、戴東霖⁵

(1)合昱工程顧問有限公司、(2)中興工程顧問社、(3)陽明交通大學土木工程學系、

(4)陽明交通大學防災與水環境研究中心、(5)經濟部中央地質調查所

自 2009 莫拉克颱風挾帶的豪雨誘發台灣中南部多處崩塌，其中尤以小林村最為周知，大規模崩塌的崩塌機制與可能影響範圍成為重要議題。經濟部中央地質調查所利用 LiDAR 高精度數值地形資料資料圈繪全台潛在大規模崩塌範圍，為能釐清坡地之破壞機制選擇以宜蘭縣大同鄉 D007 梵梵潛在大規模崩塌地為本研究場址，本場址位於蘭陽溪西側，出露地層為四稜砂岩及廬山層板岩，而牛鬥斷層為經過本研究場址的主要地質構造。

本研究試圖以多期航照立體像對判釋梵梵地區近 40 年的地表地形變化及崩塌歷史，並蒐集近年坡地災害歷史，以釐清可能的崩塌範圍。地下地質部份則進行地質鑽探及地球物理探勘，鑽探部份共進行 4 孔，鑽孔深度自 70 公尺至 100 公尺不等，總進尺達 340 公尺，提供地下岩性、崩積層、岩層分布資訊；地電阻剖面探勘共 3 條，合計長度達 1300 公尺，可參考地下崩積層與岩層界限位置，以及可能破碎帶位置。最後統整遙測判釋結果、地下調查與地表地質調查結果，建立本場址地質模式、崩塌模式及推判本區的可能崩塌歷史。

中文關鍵字：大規模崩塌



山崩與地滑地質敏感區(L1005 臺南市)變更計畫

戴東霖¹、謝有忠¹、林錫宏¹、紀宗吉¹

(1)經濟部中央地質調查所

考量近年新生山崩及中央地質調查所完成全島高解析度空載光達數值地形資料建置，以致民國 103 年 12 月 31 日公告之「山崩與地滑地質敏感區(L0005 臺南市)」原劃定範圍改變。經變更作業後，山崩與地滑地質敏感區(L1005 臺南市)已依法辦理公開展示，變更範圍位在臺南市 14 處行政區，變更後新增面積為 1.97 平方公里。

本次變更依據「地質敏感區劃定變更及廢止辦法」第 9 條「地質敏感區因環境改變或新證據發現，致使地質敏感區範圍改變時，應辦理該地質敏感區之變更」，分述如下：(1)環境改變：新增近年(103 年~107 年)之山崩記錄；(2)新證據發現：本部中央地質調查所新近產製的高解析度空載光達數值地形，提供全島山區精細的微地形資料，而能更精確劃設山崩範圍。

山崩與地滑現象常因降雨或地震事件，造成舊有崩塌範圍擴大或發生新生崩塌，以致「山崩與地滑地質敏感區」隨時間或汛期過後產生範圍變異。中央地質調查所將依據新事證，持續辦理「山崩與地滑地質敏感區」的劃定或變更，各界於土地開發前應辦理基地地質調查及地質安全評估，並研擬適當的因應措施。各目的事業主管機關應將地質敏感區相關資料，納入土地利用計畫、土地開發審議、災害防治、環境保育及資源開發之參考。

中文關鍵字：山崩與地滑地質敏感區、變更計畫、臺南市

探討綠島公館鼻安山岩磁特性

詹定勝¹、陳燕華、洪崇勝²

(1)成功大學地球科學系、(2)中央研究院地球科學研究所

綠島為北呂宋島弧的一部分，綠島大部分的岩體是由安山岩熔岩流與集塊岩所組成，偶有凝灰岩地質及碎屑岩流。本研究之樣本為綠島本島北方公館鼻 (22°40' N, 121°29' E) 的安山岩，外觀具有角閃石斑晶組織與深灰色基質，岩石硬度高深灰色岩體，為火山熔岩流產狀。經巨觀磁力(即殘磁)量測發現，該地點在距離不到 100 公尺的兩處露頭 GN163 (22°40'44.31" N, 121°29'27.12" E)與 GN168 (22°40'44.08" N, 121°29'27.01" E)，其古地磁的磁極紀錄正反各異。兩樣本之間有一界線分成上下兩處因此特別採樣。殘磁方向具有正向磁場與反向磁場(兩種磁場方向)GN163 殘磁方向為磁偏角 358 磁傾角 54(正向)GN168 殘磁方向為磁偏角 168 磁傾角 -64(反向)，藉由薄片岩象觀察與微量元素分析法，進一步了解是否為不同期火山噴發，或是其他因素而造成古地磁記錄不同。

從 X 光粉末繞射(X-ray diffraction, XRD)與光薄片觀察 GN163 主要礦物為石英(38 %)、輝石與閃石(10%)、長石類(30%)；而 GN168 中主要礦物石英(20%)、輝石與閃石(15%)、長石類(45%)；有些許樣本內含有微量黑雲母等特殊礦物(約占 5%)；而樣本中磁性礦物為鐵氧化物(約占 11%)。利用 XRD 特徵峰(35.6° (311))與 X 射線光電子能譜儀(X-ray photoelectron spectroscopy, XPS)(95% 鐵三價，5% 鐵二價)分析樣本所含磁性礦物可能為磁赤鐵礦。在電子顯微鏡(Scanning Electron Microscopy, SEM)觀察磁性礦物，顆粒大小不一最大有 100 μm 上下，最小 2-3 μm，經由能量散射光譜儀(Energy Dispersive Spectrometer, EDS)分析磁性礦物成分，分為兩大族群高鈦(19 wt%)磁赤鐵礦與低鈦(3 wt%)磁赤鐵礦，兩種磁赤鐵礦也都具有微量的鎂和鋁(1-2 wt%)。而在 GN163 與 GN168 皆有觀察到兩種磁赤鐵礦，因此化學成分可能不是影響磁性變化的主因。

而經由地球化學分析稀土元素(rare earth elements)，與未分化鐵質隕石比較，可以發現 GN168 中稀土元素濃度較 GN163 高，因此推論應該為不同期岩漿噴發所致。由於本研究磁性礦物與岩象在公館鼻兩處安山岩岩流並無顯著差異，因此推論造成兩處磁性不同的因素可能為不同期岩漿噴發紀錄所致。

中文關鍵字：綠島、磁性礦物、磁赤鐵礦、稀土元素

地震、隕石閃電(的地質紀錄)，傻傻分不清楚

郭力維¹、陳建志¹、古慶順²、蔣慶友²、Dennis Brown³、黃文正⁴、
陳則元⁴

(1)中央大學地球科學系、中央大學地震災害鏈風險評估及管理研究中心、(2)國家同步輻射研究中心、(3)Geosciences Barcelona, CSIC Barcelona、(4)中央大學應用地質研究所

極端(能量)事件，如地震破裂、雷擊與隕石撞擊，皆會產生範圍不一的劇烈破壞與影響。所以，辨識這些極端事件留下的殘跡，對地球科學、大氣科學與行星科學的研究皆有其重要性。例如，地震產生的破裂與滑移會產生假玄武玻璃(因斷層摩擦造成高溫熔融並快速冷卻之非晶質物質)，藉由解析假玄武玻璃可以萃取地震物理的資訊(能量分配，斷層機制等)，也因此，假玄武玻璃又被稱為地震化石。由於這些事件都是瞬間釋放龐大的能量於山水土石中，相對應的產物殘跡的辨識，都以高溫(超過 1000°K)、高壓(GPa)，或高溫高壓的特徵為主。目前，關於極端事件的殘跡研究，大多分析在地表採集的地質材料，根據該殘跡的產狀，以及高溫或高壓證據，多以地震破裂或隕石撞擊為機制進行討論，因為預設閃電的影響範圍很小或很淺(數公分)。本研究分析金門閃電的殘跡(又稱閃電熔岩)，顯示閃電在近地表(數公尺深)的地質材料可以造成高溫(超過 2000°K)高壓(>1.5 GPa)的特徵。該閃電熔岩(產狀與高溫特徵)與假玄武玻璃相似，而其高壓特徵與隕石撞擊造成的特徵相似。另外，模擬顯示，閃電作用可以在近地表(40 公尺深)的 10 公尺含水裂隙造成一樣的現象。所以，相較隕石撞擊與大地震，閃電是地表上好發的極端事件(地球上平均每秒 40 次落地雷)，近地表的極端事件的殘跡分析，需要將閃電作用一起考慮。不僅如此，閃電作用，也可能成為近地表地質材料中發現高壓產物的機制(例如，於西藏蛇綠岩套中發現的鑽石)。

中文關鍵字：地震、假玄武玻璃、隕石、閃電熔岩

**Electron microscopic study of smythite as a diagenetic reaction
product of pyrrhotite in methane cold-seep sediments from
Fengliao Ridge off SW Taiwan**

Ko-Chun Huang¹、Wei-Teh Jiang¹

(1)Department of Earth Sciences, National Cheng Kung University

Smythite was considered to have a formula of Fe_3S_4 and a pyrrhotite-like hcp structure intervened by a $b/6$ offset adjoining a vacant octahedral layer very 4 sulfur planes but its composition was subsequently re-determined to be Fe_9S_{11} . In this study, smythite as a reaction product of diagenetic pyrrhotite in cold-seep sediments from Fangliao Ridge off SW Taiwan was investigated by FESEM-EBSD-EDS and HRTEM. Aggregates of platy crystals of pyrrhotite or reacted pyrrhotite were identified in sediments from 7 depth intervals across the sulfate-methane transition zone at 2–3 mbsf of a 5-m sediment core. EDS analyses revealed that the replacement products of pyrrhotite included smythite (Fe_9S_{11}) and domains having smythite-like compositions and EBSD patterns unmatched with the known smythite or pyrrhotite structures. The zone-axis diffraction patterns of the EDS- and EBSD-verified smythite exhibited well-defined $00l$ and even- $h\bar{h}l$ (e.g., $\bar{2}l$) reflections indicating a periodicity of 6C (ca. 34 Å) and odd- hhl (e.g., $\bar{1}l$) reflection rows showing streaking along c^* . Such diffraction features and the periodic $b/6$ offsets of octahedral layers observed in HRTEM images partially supported the early structure model for smythite but were inconsistent with a rhombohedral lattice. In addition to the aforementioned smythite or pyrrhotite diffraction features, the EBSD-unidentifiable smythite-like domains displayed diffraction spots slightly elongated and strong streaking along c^* in the $00l$ and all of the $\bar{h}l$ reflection rows. The results implied that the Fangliao Ridge smythite had a primitive 6C structure consisting of three 2C units separated by $b/6$ offsets associated with partially occupied octahedral layers. The EBSD-unidentifiable smythite-like domains probably included interstratified layers of smythite- and pyrrhotite-like phases containing partially disordered octahedral vacancies and could be considered a transitional product for the reaction from 4C pyrrhotite to smythite.

Keywords: smythite, pyrrhotite, cold seep, electron microscopy, diagenesis

Weathering of rock fulgurite in Kinmen Island, TaiwanTze-Yuan Chen¹、Li-Wei Kuo²

(1)Department of Earth Sciences, National Central University、(2)Department of Earth Sciences,
National Central University; Earthquake-Disaster and Risk Evaluation and Management Center,
National Central University

Lightning is one of the most vigorous nature events with the typical energy of 1GJ per strike. Cloud-to-ground (CG) lightning can transmit the carried energy to the target material, resulting in an increase of temperature up to 2000 K. The target materials will (partially) melt and quench rapidly, termed fulgurite. The typical morphology of a rock fulgurite is a dozens-to-hundreds-micrometer-thick dark layer of glass, with the porosity of 5-7 area %, covering on the surface or filling in the pre-existing fractures of the host rock. However, the determination of rock fulgurite is challenging because of the absence of the glassy layer, likely due to weathering. To investigate the weathering of rock fulgurite, this study presents different field occurrences of the fulgurite relict with its remained microstructural and chemical characteristics and develops a field-based glass dissolution model to provide the time constraint. Our recent works have characterized the rock fulgurite formed in 2018, showing the distributed dark area of $\sim 10 \text{ m}^2$. On the exposed surface of the granitic gneiss hill adjacent to the rock fulgurite, several pits with different dark-crust relict ($< 0.1 \text{ m}^2$) were found, showing the consequence of weathering. Our model suggests that the 100-micrometer-thick rock fulgurite glass would take ~ 140 years to be dissolved. Our results imply that rock fulgurites are vastly under-reported due to their vulnerability to destruction and the resulting difficulty in identification. The criteria we propose to distinguish rock fulgurite relict can help to reconcile the observed frequency of lightning with the difficulty in preserving the records of ancient lightning strikes on rocks.

Keywords: Kinmen, lightning, fulgurite, glass, weathering

含水礦物熱導率對隱沒帶震測異常及其地球動力學上之應用

簡祐祥¹、謝文斌²

(1)中央大學地球科學院、中央研究院地球科學研究所、(2)中央研究院地球科學研究所

隱沒作用是將地表物質傳輸至地球內部的重要途徑。大多數的隱沒板塊曾經歷蛇紋岩化作用，此過程會透過水合作用將水儲存在含水礦物中，以穩定地傳遞到地函深部。夾帶大量含水礦物的板塊在隱沒過程中隨溫度上升開始脫水作用，這些釋放出的水將會對圍岩的物理性質有顯著的影響。然而，控制隱沒帶溫度變化並觸發礦物脫水的機制目前還缺乏完整的研究。我們將以 $\text{MgO-H}_2\text{O-SiO}_2$ 成分系統中橄欖石、蛇紋石、水鎂石的熱導率為例，結合超快速光學與鑽石高壓砧量測礦物於高壓下的熱導率，透過研究含水礦物熱導率的變化如何影響隱沒板塊的溫度剖面，為礦物脫水機制與其對震測觀察中的影響提供新的見解。

我們發現在隱沒至約 200 公里深時，蛇紋石的熱傳導率會受晶體方向性影響，在假設 10 公里厚的蛇紋岩層中產生約 $7 \text{ W m}^{-1} \text{ K}^{-1}$ 的差異，並使板塊中的地溫梯度上升約 50 K。由於蛇紋石的脫水行為對溫度很敏感，這可能會影響到由流體觸發地震的發震位置。部分脫離板塊的蛇紋石塊體，也容易在此深度產生脫水反應並形成該區域的速度異常，此結果將有助於我們解釋 Lehmann 不連續面的成因。此外，由蛇紋石晶體順向排列所形成的低熱導帶也有可能使部分含水礦物能存活至較深的深度，此結果有助於探討地球深部水循環的傳遞路徑。最後，在隱沒到下部地函頂部約 800 公里深處，板塊中由水鎂石富集的區域會分解成方鎂石與液態水，並導致熱導率突然增加約 9-16 倍。此熱導率不連續所造成的板塊溫度異常升高(約 100 K)將改變整體板塊密度與浮力，從而促進板塊滯留在該深度。同時釋出的水也可能遷移並富集在下部地函頂部形成震波低速帶。

中文關鍵字：含水礦物、脫水作用、熱導率、震測異常、隱沒帶

A high strain shear zone in the metamorphic core of Central Range, Taiwan: A possible Plio- Pleistocene transform fault

Gong-Ruei Ho¹、Timothy B. Byrne²、Jian-Cheng Lee¹

(1)Institute of Earth Sciences, Academia Sinica, Taiwan、(2)Department of Natural Resources and Environmental Studies, National Dong-Hwa University

The young and presently active Taiwan orogeny provides an excellent tectonic “scene” for studying orogenic processes. In this study, we propose the structures preserved in the Tailuko Belt record oblique, left-lateral convergence, which was mainly driven by the northward movement of the Philippine Sea plate wrt the Eurasian plate. A penetrative foliation, S2, that includes mylonitic and gneissic fabrics, dips moderately WNW and is associated with a sub-horizontal stretching lineation, L2. Hundreds of kinematic indicators from 6 rivers and along-strike transections of relatively high strain are particularly well-developed and include: asymmetric folds, strain fringes around pyrite ore magnetite, S-C fabrics, en échelon veins, R and R’ shears, sigmoidal core-and-mantle structures are identified top-to-southwest sense of shear. In cases where the L2 asymmetry could be determined 80-90% yielded a left-lateral sense of shear. A synthesis of available data suggests that a previously unrecognized zone of strike-slip deformation exists in the Tailuko Belt, and here we document: 1) the distribution of horizontal shear, 2) the kinematics of deformation, 3) the age of deformation and 4) regional consistency between geologic studies and plate reconstructions. We also present a 3D model and discuss the impact of horizontal shear in the shallow structural level of southern Taiwan (e.g., Taimali River and Hengchun Peninsula areas) where previously published kinematic data argue for CCW block rotations. Later deformation events are also recorded in the metamorphic core and cover sequences and are responsible, in part, for tilting of S2 from an initial sub-vertical orientation (Byrne and Chojnacki, this session). Finally, we integrated these field-based observations with data from the Slate Belt and propose that during the development of S2 plate convergence was partitioned into orogen-parallel motion in the Tailuko Belt and orogen-perpendicular in the Slate Belt.

Keywords: Yuli Belt, left-lateral shearing, deformation fabrics, ductile shear zone

Tectonic exhumation (and erosion) of a metamorphic core in the Pleistocene, Taiwan

Tim Byrne¹、Michael Chojnacki²

(1)Department of Natural Resources and Environmental Studies, National Dong-Hwa University、

(2)USEngineering Solutions Corp.

We propose that extension and thinning of the upper crust, i.e., tectonic exhumation played a significant role in exhuming the metamorphic core in Taiwan. The youngest penetrative fabric in the metamorphic core, S_3 , forms a broad, gently NE plunging antiform. The cleavage is also typically axial planar to numerous recumbent folds, suggesting significant vertical shortening. Veins of quartz, calcite, albite, and/or adularia appear mildly deformed by S_3 , suggesting development late in the formation of S_3 . The veins ($n=92$) strike NW-SE, dip steeply, and are generally normal to the mineral stretching lineation, which plunges NE. In X-Z sections, asymmetric structures are weakly developed and suggest top-to-NE or top-to-SW shear. Fluid inclusions in euhedral to subhedral crystals of quartz and adularia suggest entrapment temperatures of 200°C to 350°C. Ar^{40}/Ar^{39} dating of the adularia suggests crystallization at ~2.5 Ma (see also Chojnacki, MS thesis, 2019). P-T conditions, geometry, and kinematics of S_3 are similar to conditions documented for pseudotachylite exposed along the Hoping River (Korren et al., 2017) which yielded a 1.5 Ma Ar^{40}/Ar^{39} age (Chen et al., 2017). We propose that the pseudotachylite represents the waning stages of S_3 -related exhumation.

The low dip and regional extent of S_3 argue for significant vertical shortening and/or substantial sub-horizontal shear strain. We prefer a top-to-the northeast shear during S_3 because this sense of motion provides a mechanism for deforming S_2 from an initial vertical orientation (see Ho et al., this session) to its present moderate WNW dip. Top-to-the northeast motion also implies that the metamorphic core was tectonically exhumed from beneath the Luzon forearc. We propose that tectonic exhumation occurred from about 2.5 Ma to at least 1.5 Ma, the time of rapid exhumation cooling in the core (Hsu et al., 2016). The relative importance of tectonic versus erosional exhumation is an important topic for future research.

Keywords: exhumation, Tailuko Belt, erosion

以熱變質度解析台灣中部雪山－脊梁板岩帶邊界構造運動模式

陳尚謙¹、陳致同¹

(1)中央大學地球科學系

在台灣造山帶中，板岩帶為被動大陸邊緣不同部位沉積物之深埋、隱沒、變質，最終掘升至地表之結果，其中以梨山斷層為界，可再劃分為雪山板岩帶與脊梁板岩帶，二者之地質年代、變形行為、變質度皆有所落差。因此若要對板岩帶，以至於台灣造山歷史有更一步的剖析，作為界線斷層的梨山斷層有不可忽略的研究價值。本研究以拉曼碳質物光譜(Raman Spectroscopy of Carbonaceous Material, RSCM)進行板岩帶變質巔峰溫度(T-peak)高密度量測。RSCM 為一高精度 T-peak 溫度計，其樣本間誤差值可低至 10-15°C，對區域的 T-peak 變化能有更精準的結果。本研究區域於中橫梨山段向北延伸至啞口一帶，界定出雪山-脊梁交界處 T-peak 有約 45-60°C 的陡降。此外預計將 T-peak 結果結合薄片微構造觀察及野外斷層擦痕資料，推論梨山斷層可能的位置、運動模式及變形歷史。

中文關鍵字：拉曼碳質物光譜、梨山斷層、雪山山脈、脊梁山脈板岩帶



從盆地到山脈：整合地層架構與變質沉積岩熱歷史

陳致同¹、張簡婉晴¹、孫浩誠¹、阮氏秋河¹、陳尚謙¹、阮氏金庸¹

(1)中央大學地球科學系

造山帶由海洋隱沒轉進大陸俯衝而形成，洋盆與大陸邊緣上的沉積蓋層經常隨之經歷複雜構造運動並廣泛出露：從山脈外緣褶皺逆衝帶的未變質層序，到山脈內部的變質沉積岩，呈現不同的層序-變質度關係。如此沉積盆地構造反轉的過程反映了造山作用的機制：下覆板塊的岩石材料是於地殼淺部受擠壓即進入褶皺逆衝帶而抬升(前緣加積作用/frontal accretion)，抑或是經歷不同程度的俯衝與構造深埋而後才於深部進入山脈增積體/orogenic wedge (底部加積作用/basal accretion)。藉由詳細比對沉積岩於造山前沉積盆地內的埋藏和其最高變質度，可判定同造山的變質作用的存在與否及強度，指示其進入造山帶的機制；進一步比對褶皺斷層構造中的層位與最高變質度，比較山脈不同部位變形與變質作用的相對年代關係，從而解析合理的底脫面斷層幾何等山脈架構。於東亞地區數個現生與古老造山帶岩石熱歷史分析的初步工作顯示，變質沉積岩是山脈增積體的主要組成，並經由底部加積作用貢獻了大量的地殼增厚，指示了底脫斷層等主要構造的多變與複雜性。

中文關鍵字：岩石熱歷史、增積造山楔、碳物質地質溫度計、台灣造山帶



Extensional tectonics for basement uplift of the Fansipan and Tule mountain ranges in northern Vietnam

Dinh Thi Hue¹、Yu-Chang Chan¹、Chih-Tung Chen²

(1)Taiwan International Graduate Program (TIGP) – Earth System Sciences Program, Academia Sinica and National Central University; Institute of Earth Sciences, Academia Sinica, Taiwan、

(2)Department of Earth Sciences, National Central University

Located in northern Vietnam, the Fansipan and Tule mountain ranges are high topography regions adjacent to the strike-slip Red River Fault, an important structure related to the India-Eurasia collision. How the mountain height is maintained today under humid subtropical climate is important to improve knowledge about tectonic deformations of northern Vietnam and may have broader implications on crustal dynamics of circum-Tibet regions. We therefore utilized observations from the field and digital elevation model (DEM) data, and topographic analyses to constrain active fault systems that likely contributed to the uplift of the mountain ranges. Our observations from DEM and field data indicate possible active normal and strike-slip faults within and surrounding the Fansipan and Tule mountain ranges such as: the Phong Tho-Nam Pia fault, the Tule fault, and the Nghia Lo fault. In addition to these observations, the results from geomorphic indices including both the stream-length gradient index (SL) and the normalized steepness index (k_{sn}) present high values of indices in the footwalls of the inferred normal faults and the low values of indices in the hanging walls. Furthermore, most of identified knickpoints are related to the locations of the mapped faults. The correlation of these data indicates that recent movements of the Fansipan and Tule mountain ranges area dominated by strike-slip and normal faulting under extensional tectonics. We therefore proposed that the extensional tectonics likely play a role for isotactic rebound that maintains the mountain height for a long time in spite of continual erosion in the monsoon-affected areas.

Keywords: Fansipan and Tule mountain ranges, stream-length gradient index (SL), normalized steepness index (k_{sn})

Buchan type metamorphism in the Pingtan-Dongshan Metamorphic Belt, SE China: Evidences from combined EMP monazite and U-Pb zircon ages of mica schists

Jian-Wei Lin¹、Chi-Yu Lee¹、Cheng-Hong Chen¹、Takenori Kato²、
Yuji Sano³、Takahata Naoto³

(1)Department of Geosciences, National Taiwan University、(2)Institute for Space-Earth
Environmental Research, Nagoya University, Japan、(3)Atmosphere and Ocean Research Institute, the
University of Tokyo, Japan

Detailed age information of the Pingtan-Dongshan Metamorphic Belt in the coastal Cathaysia Block is important in understanding geodynamics of South China continental margin. Geochronological determinations on monazite and zircon inclusions and zircon separates from five mica schists, the most representative rock type in this belt, and two granites intruding schists are studied. Ages of monazite and zircon inclusions within index constituent minerals (quartz, muscovite, sillimanite and K-feldspar) in all schists define a significant peak age at ~100 Ma for the high temperature/low pressure metamorphic event. Along with zircon ages of granites (106 and 101 Ma), a Buchan type metamorphism is proposed regarding heat source from the post-orogenic magmatism in the neighboring igneous province. For discrete zircons, age distribution patterns identify two groups of schist that suggest separated provenances of sediments prior to metamorphism. One group has a simple age cluster (145-130 Ma) inferring proximal Early Cretaceous magmatic rocks in the Cathaysia. Contrarily, another group shows a widespread time span containing two particular age populations of ~1.8 Ga and ~190 Ma that are uncommon in the Cathaysia but comparable to schists in the Tailuko Metamorphic Belt of eastern Taiwan. This suggests an extra provenance between these two belts and a now-concealed microcontinent would play such a role. Accordingly, we advocate a new tectonic framework of this belt that involved two different provenances of sediments and its configuration was influenced by a high temperature regime caused by mantle upwelling as a reflection of slab rollback of the subducted Paleo-Pacific Plate.

Keywords: U-Pb zircon age, EMP monazite age, mica schist, Pingtan-Dongshan
Metamorphic Belt, Cathaysia Block

From diagenetic to anchizone, a transition of the very-low metamorphism zones in progressively emerging and exhuming orogen in the southern Taiwan, Hengchun Peninsula.

Jack Giletycz¹、Andrew Tien-Shun Lin¹、Li-Wei Kuo¹

(1)Department of Earth Sciences, National Central University

Southern Taiwan (Hengchun Peninsula) characterizes topography that has been recently emerged above the sea level. Because of that, the surface has been exposed to subaerial process as erosion, landscape reorganization and sediment outflux. As the result, the Hengchun Peninsula might reveal initial exhumation processes and therefore-outcropping first stages of a low-grade metamorphism. Illite crystallinity and X-ray diffraction were used to survey the central and northern Hengchun Peninsula to indicate a potential pattern of this exhumation. 32 samples from sites across the Hengchun Peninsula were collected. Küber Index (KI) derived from the first peak of the FWHM (full-width half-maximum) of the illite diffraction revealed a low anchizone of the very-low metamorphic grade in an asymmetrical pattern shifted to the east. The field structural measurements also show a similar pattern of the advancing deformation from mudstones to argillites exposing pencil cleavage, then slaty cleavage and even first indication of boudinage and crenulation cleavage in the northmost part of the Hengchun Peninsula. These results coupled with a geological map gives a new insight into local geology and tectonic setting of the southern Taiwan.

Keywords: very low metamorphic grade, exhumation pattern, southern Taiwan, Hengchun Peninsula

Structural evolution and activity of Kirkuk recess in Zagros orogenTing-Yun Lee¹、Jyr-Ching Hu¹、Kuang-Yin Lai²、Ping-Jung Hsieh²

(1)Department of Geosciences, National Taiwan University、(2)Exploration and Development

Research Institute, CPC Corporation

Zagros orogen is part of the Alpine-Himalayan orogenic system and is formed as a result of collision between Arabian Plate and Eurasia Plate with a convergent rate of about 22 mm/yr. Foreland basin of Zagros orogen is one of the most important petroleum-rich area in the world. Kirkuk recess in the northwestern part of the Zagros orogen contains 18% of oil and gas storage of the whole foreland basin. Therefore, a more complete understanding of structural evolution should be helpful to increase the accuracy of oil and gas exploration. This study can be divided into two parts, first we use MOVE 2018 software to restore the balanced cross section in order to investigate the structural evolution of Kirkuk recess. Initial length of the cross section is about 212 km, and gives shortening around 16.3 km after the restoration, 7 km of them being accommodated within the Inner High Folded Zone. The result shows that the deformation propagated from northeast to southwest, which reflects the in-sequence evolution of the low angle basement-rooted thrusts. Because these thrusts don't penetrate the sedimentary cover but connected upward to the basal detachment layer, shortening caused by uplift were propagated to foreland and finally formed detachment folds in sedimentary cover. As the result, deformation style in the study area is characterized by multi-detachment folds detached above a basal detachment level. In the second part of the study, we use Small Baseline Subset (SBAS) technique to deal with D-InSAR data, in order to analyze temporal surface deformation across main fault-related folding within three years. The result shows that hanging wall of Mountain Front Fault have downward movement one year after the 2017 Mw 7.3 earthquake and this implies that Mountain Front Fault continued to slip after the mainshock, thus caused extension on the hanging wall. As the result, we consider Mountain Front Fault is still active nowadays. After realizing structural evolution from the beginning of orogeny and current structural activity, we can have more comprehensive explanation of deformation style in Kirkuk recess.

Keywords: balanced cross section, Zagros orogen, Kirkuk recess, InSAR, small baseline subset

微震監測與應力反演：在 2018 花蓮地震與 2019 地震之前

吳瑋哲¹、蘇建旻¹、溫士忠¹、李奕亨²、廖彥喆²、彭筱涓²、
陳俊榕²、陳朝輝¹

(1)中正大學地震學研究所、(2)工業技術研究院綠能與環境研究所

2020 年，由於新冠肺炎的流行，使得過去進行地球科學研究的模式，遭遇到很大的困境。本研究希望藉由精確的利用過去於應力研究中常被捨棄不用的微震事件，來獲取一些過去所無法得到的一些資料，近而能夠更為詳細的了解該區域的孕震構造以及背景應力狀態，透過三維速度構造的重定位、波線追跡技術，以及全事件的應力反演方法，本研究能夠更為客觀且更精準的運用地震資料，確保資料非由於人為主觀意識所影響，並引入了信賴區間的概念，近而提高所得結果之可信度。結果顯示，台灣東北部地區其孕震構造皆受到菲律賓海板塊隱沒以及沖繩海槽開張之複合式影響，地震活動複雜，未來可透過微震資料的增加，透過微分區的方式，仔細的去了解該區域之孕震構造於空間上的分佈，並提供未來進行應力轉移研究時，所需相關背景應力資訊。

中文關鍵字：台灣東北部、應力反演、微震監測



利用地震活動分布與 P 波速度構造建置西部麓山帶滑脫面

三維幾何模型

范秋屏¹、陳冠宇¹、張毓文¹、張志偉¹、劉勛仁¹

(1)國家地震工程研究中心

臺灣西部麓山帶的活動斷層構造其地下形貌極其複雜，即使透過地球物理探勘方法與地震學理論模式，仍難以清楚釐清並描繪此區孕震構造位置與活動斷層間之相互關係。有鑒於此，若能建立一套西部麓山帶滑脫面之三維幾何模型，將有助於了解此區複雜的斷層幾何構造形貌。

地質學家建立平衡剖面來重現斷層-褶皺帶的地下形貌及壓縮量，用以解釋淺部地殼變形的演化過程，而臺灣西部褶皺逆衝帶與逆衝斷層系統因受板塊擠壓驅動、由東向西成覆瓦狀排列；在薄皮理論架構下，構造變形多發生於深度約 10 公里內的淺部地層，平衡剖面裡可見一個向東傾斜且低傾角的介面，即為滑脫面，此介面為塊體間的弱面，在壓縮過程中，可能以頻繁的小規模地震釋放能量，Carena et al. (2002)應用當時地震資料庫的小規模地震建置滑脫面的三維幾何，但較為粗略，且未與其他區塊整合成一連續的滑脫面模型。

隨著地震解析技術的提升，現今的地震目錄精度將有助於探討滑脫面的空間位置。本研究嘗試以密集繪製的地震分布剖面並利用網格化的方式建立滑脫面三維空間幾何形貌。研究區域參考南北走向之西部活動斷層的空間分布，在臺灣中部海岸平原區及麓山帶框定東西跨距 90 公里、南北跨距 150 公里的範圍，並在研究區域內以 5 公里等間距繪製 2 組互相垂直的地震分布剖面。前人研究中 (Davis et al., 1983 ; Huang et al., 2004 ; Mouthereau et al., 2006 ; Simoes et al., 2007) 說明，西部麓山帶的滑脫面係約為一向東傾約 6 ± 1 度的面，本研究依此作為初始模型在前述的地震剖面上套疊，以建置滑脫面的初步模型。為能進一步探討初步模型之合理性，本研究另參考 P 波速度構造分布 (Kuo-Chen et al., 2012 ; Huang et al., 2014) 與震源分布一起檢視所有剖面中滑脫面的位置，結果顯示滑脫面位置與 P 波速度約 5.2km/s 分布大致相符 (Camanni et al., 2016 ; Brown et al., 2017 ; Biete et al., 2018)。雖因地震資料上的限制，滑脫面與 P 波速度構造上存在差異性，但判斷下最終能取得本研究區域內所有剖面中之滑脫面深度數值，最後利用 GIS 軟體建置初版的西部麓山帶連續滑脫面三維幾何模型。

臺灣西部的褶皺逆衝斷層帶，因地質構造複雜，對斷層系統的三維幾何建置充滿挑戰，本研究認為先定義出滑脫面的位置有助於整合研究區域內的斷層幾何模型，不僅可作為斷層幾何在深度方向延伸的邊界，更能有效排除相鄰斷層間幾何形貌的衝突性，後續可與地調所發布的活動斷層作討論，以利更了解臺灣西部麓山帶的活動斷層三維幾何模型。

中文關鍵字：滑脫面、地震分布剖面、西部麓山帶、地理資訊系統



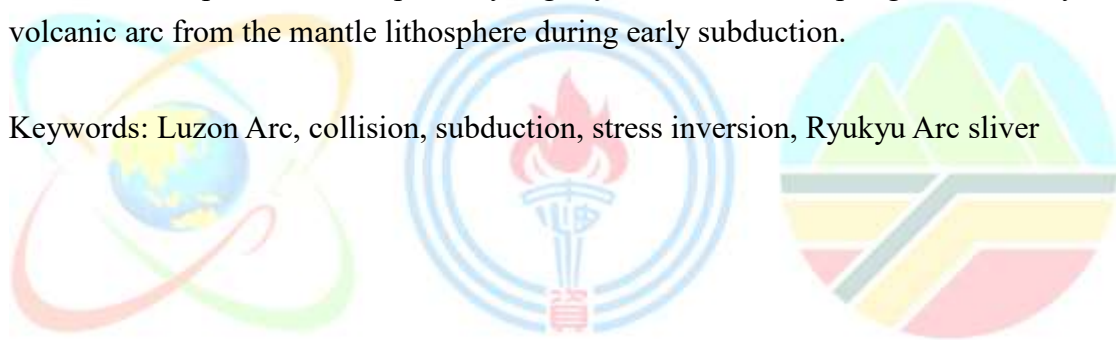
Fate of the Luzon Arc after subduction: Evidence from stress inversion along the Taiwan collision boundary

Ban-Yuan Kuo¹、Pei-Ru Jian¹、Wen-Tzong Liang¹

(1)Institute of Earth Sciences, Academia Sinica, Taiwan

The arc–continent collision boundary of Taiwan involves complex deformation that is difficult to visualize using conventional two-dimensional stress analyses. We employed a three-dimensional spatial clustering approach in eastern Taiwan to reveal how stress varies along the collision boundary. Results show that the maximum horizontal compression orientation, SH, is parallel to the plate motion throughout the boundary at all depths except in the crust of the northern segment, where SH exhibits a clockwise rotation from convergence-parallel by up to 30°. Concurrent with the SH rotation, the maximum compressive P-axes steepen in the same crustal segment. We interpret this phenomenon as resulting from the rotation of the stress regime in the crust of the Luzon Arc forced by the bending of the Ryukyu Arc continental sliver. The differential response with depth may signify an initial decoupling of the buoyant volcanic arc from the mantle lithosphere during early subduction.

Keywords: Luzon Arc, collision, subduction, stress inversion, Ryukyu Arc sliver



Revealing seasonal crustal seismic velocity variations in Taiwan with single-station cross-component analysis

Kuan-Fu Feng¹、Hsin-Hua Huang²、Ya-Ju Hsu²、Yih-Min Wu¹

(1)Department of Geosciences, National Taiwan University、(2)Institute of Earth Sciences, Academia Sinica, Taiwan

Ambient noise interferometry is a promising technique for providing continuous measurements of seismic velocity changes (dv/v) and studying crustal behaviors in relation to various geophysical processes over time. In addition to the tectonic-driven dv/v changes, dv/v is also known to be affected by environmental factors through rainfall-induced pore-pressure changes, air pressure loading changes, thermoelastic effects, and so forth. In this study, benefiting from the long-term continuous data of Broadband Array in Taiwan for Seismology (BATS) that has been operated since 1994, we investigate the evolution of crustal seismic velocity by applying the single-station cross-component (SC) method on the continuous seismic data from 1998 to 2019. We construct the noise correlation functions and compute daily seismic velocity changes by the stretching technique in a frequency band of 0.1 to 0.9 Hz. In our dv/v results, we observe the co-seismic drops associated with inland moderate earthquakes and also the clear seasonal cycles that appear at most stations but with different characteristics. Systematic correlational analyses with the weather data suggest that the rainfall-induced pore-pressure change is likely the main cause of the seasonal variations with high correlations. The observed site-dependency of these seasonal dv/v variations implies spatially-varying complex hydro-mechanical interaction across the orogenic belt in Taiwan.

Keywords: seismic velocity change, single-station cross-component method, stretching technique, seasonal variation

初探台灣高階噪訊表面波的時空特性

廖峻甫¹、陳映年¹、陳昱安¹、黃有志²

(1)中正大學地球與環境科學系、(2)國家地震工程研究中心

地震學中的噪訊(microseisms)主要源自於海浪與沿岸或是海床的能量交換，其傳遞方式多以基態(fundamental mode)表面波為主，只有在特殊天氣系統或海床構造下，才有機會產生體波或是高階(higher-mode)表面波的噪訊能量。透過噪訊干涉法，除了可以提供高密度的表面波格林函數來進行速度構造相關的研究之外，也可以進一步釐清噪訊源的時空特性。根據研究指出，由於台灣周遭海浪週期約為 7-9 秒，因此可以提供以基態表面波傳遞為主高頻的次級微震(secondary microseism, 2-5 sec)，且激發能量與季風系統與水深有關。近年來將干涉技術應用在多分量的噪訊紀錄上，很多研究發現干涉波形中出現高階(higher-mode)表面波，且其起源可能與沈積層的基盤有關。台灣西部以沈積構造為主，往東進入板塊碰撞造山帶，劇烈的側向構造變化，提供很好釐清噪訊高階表面波起源的試驗場所。為了探討高階噪訊表面波空間分佈特性與地質構造的關係，本研究結合 CWB、BATS 與 TSMIP 三個地震觀測網的資料，以提升干涉波形在空間上的解析能力。透過分析干涉波形的質點運動與表面波頻散曲線，可以清楚分辨基態與高階表面波的訊號。我們將測站依照地理位置加以分組，透過干涉波形的非對稱性與 Beamforming 的結果，發現高階噪訊表面波的空間分佈特性與台灣構造息息相關。未來將結合高階與基模噪訊表面波的 H/V 特性與頻譜特徵，勾勒西部沖積平原基盤的幾何樣貌。

中文關鍵字：噪訊、干涉法、高階表面波

觀測大屯火山地區流體上升現象

蒲新杰¹、林正洪²、李曉芬³、賴雅娟³、張麗琴³、史旻弘³

(1)中央氣象局、(2)中央研究院地球科學研究所、(3)國家地震工程研究中心

近年，關於大屯火山的構造研究十分多樣化。這些研究的重點，點出了大屯火山淺層的火山構造特性，例如壓力源構造、火山流體上升的位置、火山流體的成份來源、火山流體形成的特殊地動訊號…等。這些研究不但指出了大屯火山的活動性，同時也表明了其可能形成的威脅。與之不同之處，在於本研究將試圖以現有的資料，探討如何監測這些流體的變化。使用的資料有地震與火山噴氣的成份，這些資料的來源為大屯火山觀測站。基於過去的研究可知，大屯火山的大油坑下方可能存在一個壓力源，而大油坑地區的噴氣成份又被推測可能包含了火山特性。基於這個模式，本研究分析大屯火山地區的地震震源機制，進一步將震源機制分成正、逆、走向滑移等三種機制。進一步再分析在壓力源週邊與壓力源上方地區的震源機制型態隨時間的變化，結果發現，在壓力源周邊的逆斷層發生率與壓力源上方的正斷層發生率有極高的相關性與些許的時間差，而這些時間變化又與地表的噴氣成份中的硫含量變化趨勢相仿。基於這些觀測資料，本研究推出了大屯火山地區的火山流體上升模式。而三種觀測資料間的時間差，正好反應了火山流體上升的位置。此結果在火山監測中，具有極高的應用性。因為這些觀測資料可以在可能造成災害的火山流體傳播至地表產生噴發前，約4個月前，預先監測到流體活動。這個時間段，讓監測單位有時間可以多方確認各項資料，同時發出預警資訊。

中文關鍵字：大屯火山群、上升流體、震源機制、火山噴氣

深度學習於地震偵測之落地化：連續資料的波相挑選及

降低反投影法之計算開銷

廖勿渝¹、李恩瑞¹

(1)成功大學地球科學系

近來，深度學習算法於地震學之嘗試如雨後春筍冒出，而如何將演算法納入連續，甚至是即時的地震資料處理流程是值得被關注的議題。為了提高模型在動態的波形上偵測地震及波相的穩定性，我們提出了 Marching Mosaic Waveform Augmentation (MMWA)。在模型的訓練資料中加入以不同地震波形拼接而成的資料，並使其隨機前後移動，以模擬多組地震訊號同時出現，以及在判釋的時間窗格內被截切的狀況。本研究以在固定時間窗格內判釋地震 P 波及 S 波到時的模型為例，在時間域上對所有資料點進行移動式的重複判釋，取其中位數以作為模型的穩定輸出。此判釋方式能迫使模型判釋每個資料點時，能同時注意其他資料點隨著時間變化的情形，以模擬人類判釋地震波相到時的行為。反投影法(back-projection)藉由在連續資料上針對多個測站所記錄到的特定訊號（如初達 P 波）建構特徵方程式（如 STA/LTA, Kurtosis 等），在時、空間域進行疊加，以尋找潛在的訊號源。使用傳統的線性方法建構特徵方程式，在連續資料的處理上最大的問題有三：(一)無法分辨 P 波、S 波。(二)無法捕捉在短時間內連續發生之地震，尤其是振幅差異較大之事件。(三)特徵方程式的值無統一單位，偵測閾值設定困難。因此在實務應用上，在地震記錄的三個分量上分別對 P 波及 S 波設計特徵方程式，並使用研究區域的 P 波及 S 波速度模型分別進行演算再疊加是較保守的做法。然而地震波形的變異性甚大，無法以同組參數量化所有地震出現時，所有波相的特徵。本研究以兩百萬餘筆三分量地震記錄(約 5%純噪音，約 25%為 MMWA 所合成的資料)訓練而成的 ARRU (Attention Residual-Residual U-Net) seismic phase picker 進行連續資料的地震偵測及波相判釋，可以很好的緩解上述三個困境。此外，將需要建構並疊加的時間序列函數減少為原本的三分之一，即只輸入模型所產出的 P 波及 S 波偵測函式。其中最大值為 1，最小值為 0，演算法的數值穩定度較高。

中文關鍵字：深度學習、地震偵測、波相挑選、資料增強、連續資料處理

From two-class to one-class classification of tectonic tremor in Taiwan

Yu-Siang Wu¹、Ting-Chen Yeh¹、Kate Huihsuan Chen¹、Yi-Hung Liu²

(1)Department of Earth Sciences, National Taiwan Normal University、(2)Department of Mechanical Engineering, National Taiwan University of Science and Technology

In Taiwan, ambient tremors are found to locate underneath a mountain in Southern Central Range. Given that the ambient tremors represent the aseismic slip process at greater depth where no seismicity is present, it is crucial to monitor their activity. To identify tremors, the similarity and time lapse of the arrival tremor bursts from multiple stations are oftentimes demanded, while manual checks of multi-station waveforms are practiced, to exclude loud noise and swarms of regional earthquakes.

We aim at exploring if the advances of machine learning techniques enable an automatic search for patterns to discriminate tremor from regional earthquakes. Using *k*-Nearest Neighbor (*k*-NN, Cover and Hart, 1967) classifier, Liu et al. (2019) successfully separated tremor from local earthquakes and noise at high accuracy of 86.6-98.8%, showing that the possibility of applying ML technique to separate tremors from other types of seismic signals is feasible. However, they also found that the multi-class classification approach is not robust in the real-time monitoring using continuous data. This is mainly due to the fact that in the continuous data, many other types of signals exist without being labeled. In this study, not only two-class but one-class classifier was built to test if tremor can be separated from regional earthquakes and the possibility of continuous tremor detection.

Using 5,796 tremor, 6,746 regional earthquake, and 441,887 noise data collected in 2016, we found the two-class *k*-NN classifier allows the high classification rate (CR) of 91.8-95.8%. We further demonstrate the performance of one-class Support Vector Data Description (Tax and Duin, 2004) classifier that does not need a collection of other classes' samples. The resulting CR of 71.1-82.8% indicates the capability of one-class classifier on real-time detection of tremor in Taiwan.

Keywords: tectonic tremor, machine learning, real-time detection, Support Vector Data Description

科技部地化儀器平台-大體積壓力機及現地高溫高壓拉曼

龔慧貞¹、王筑萱¹、王曜睿¹、李孟旋¹、林秋婷¹、莊勝智¹、
郭琢琪¹、黎靜謙¹、蘇毓婷¹、蕭賢義¹

(1)成功大學地球科學系

成大礦物物理實驗室在科技部地化平台計畫及成功大學支持下，安置 1000 噸大體積壓力機及拉曼光譜儀。目前 1000 噸大體積壓力機做為提供高溫高壓的實驗環境來模擬地球內部環境合成地函樣品，以供不同的實驗研究。另一方面也提供不同領域,如材料、物理及化學，延伸「壓力」維度在合成/研究新穎材料。除了合成實驗，大體積壓力機也可用於一些現地高壓實驗如電阻量測。拉曼光譜儀提供物質快速鑑定便利及可以提供非破壞的檢測，這儀器在許多地質實驗室多有安置。我們藉拉曼光譜反映晶體結構的關係，也可在無 X 光單晶繞射儀裝置，對自型或半自型單晶的晶軸快速鑑定，應用在單晶物理性量測。也將拉曼光譜儀結合鑽石高壓砧和高溫加熱台，來研究物質在高溫高壓下的晶體動力學和相變行為的現地實驗。這些研究結果可用來探討化學成分和物質性質與其如何影響地球內部之行為或材料之物理性質。我們將在本會議介紹大體積壓力機及高溫、高壓拉曼光譜實驗及報告實驗結果應用。

中文關鍵字：大體積壓力機、拉曼、晶體動力學、相變



Evaluation of nano-particulate pressed pellet reference materials of igneous rocks by micro-X-ray fluorescence spectrometry

Kwan-Nang Pang¹

(1)Institute of Earth Sciences, Academia Sinica, Taiwan

Micro-X-ray fluorescence spectrometry offers a potentially efficient way of quantification of major and minor elements in rock samples. However, variables like accuracy, precision and lower limit of detection have not been widely addressed, hampering its direct application. In this study, I evaluate six nano-particulate pressed pellet reference materials of igneous rocks manufactured by myStandard GmbH, including OKUM (komatiite), BHVO-2 (basalt), BCR-2 (basalt), BIR-1 (basalt), GH (granite) and AC-E (granite), by bench-top micro-X-ray fluorescence spectrometry (Bruker M4 Tornado Plus). Analyses were performed with X-ray beam size of $\sim 20\ \mu\text{m}$ in a controlled vacuum by two different ways: (i) averaging >15 spots in a grid on the sample with measurement time of 120 seconds per spot, and (ii) averaging X-ray spectra collected over a rectangular area on the sample with measurement time of 20 milliseconds per pixel. X-ray intensity was converted to elemental concentration by fundamental parameter-based standardless quantification, and data obtained by both ways correlate very well. I also find that fundamental parameter-based standardless quantification is only accurate for some elements, as reported in recent investigations, with P_2O_5 showing the greatest discrepancy among the ten major oxides commonly reported for igneous rocks. Accuracy, however, could be improved by calibration based on the reference materials analyzed, as demonstrated by analysis of samples independently verified by conventional major element analysis. Precision, which is examined by deviation from the mean of the spot analyses noted above, is good for all reference materials analyzed, and lower limit of detection is found to be element-dependent. Overall, micro-X-ray fluorescence spectrometry is promising for rapid determination of major and some minor elements in igneous rocks, particularly when sample quantity is limited.

Keywords: micro-X-ray fluorescence, geochemistry, igneous rocks, pressed pellet, quantification

泥炭岩心 ^{14}C 定年以及地球化學指標問題

李紅春¹、張海龍²、孫晶晶³、周春燕¹、張庭漪¹

(1)臺灣大學地質科學系、(2)中國海洋大學教育部海洋理論和技術重點實驗室、

(3)中國東北師範大學地理科學學院

泥炭岩心是重建古氣候和古環境以及研究碳循環的重要材料。儘管過去有研究建議泥炭岩心的定年樣本應該選用生長在空氣中（而非水面下的）的苔蘚，但實際上苔蘚很容易分解，在岩心中不易選到，要選到特定長在水面之上的苔蘚更是難上加難。因此，絕大多數泥炭定年是將混合植物殘體用於 ^{14}C 定年。通常泥炭 ^{14}C 定年結果基本符合年齡層序，一根幾米長的岩心用 4-5 個定年結果計算岩心柱年代。然而，在我們近幾年的研究中常常發現高密度泥炭岩心定年發生年齡倒序。同時，許多過去的泥炭同位素記錄都是採用總植物中提取的纖維素測量來重建古氣候和古環境。泥炭植物中不僅包括苔蘚、草本、木本三大類，而且每一類中又有多種不同種類的植物，其同位素值相差很大。古氣候和古環境指標是否能用這種混合植物的泥炭同位素記錄代表，是值得商榷的。為此，我們從中國長春哈尼和金川泥炭地獲得不同種類的泥炭植物進行 ^{14}C 定年、碳氮含量和 ^{13}C 測試，討論泥炭定年和指標問題。2018 年從哈尼泥炭地採集的 18 種現生不同植物包括 5 種苔蘚，5 種草本和 8 種木本。這些植物分析結果顯示， $\delta^{14}\text{C}$ 、 $\text{N}\%$ 、 $\text{C}\%$ 、 C/N and ^{13}C (‰ VPDB) 的平均值和標準偏差分別為 5 種苔蘚 1.0159 ± 0.0082 、 0.90 ± 0.10 、 44.39 ± 1.41 、 49.5 ± 4.5 、 -27.20 ± 0.58 ；5 種草本 1.0104 ± 0.0141 、 2.06 ± 0.88 、 47.85 ± 2.95 、 25.7 ± 8.5 、 -21.18 ± 5.26 和 8 種木本 1.0082 ± 0.0092 、 2.52 ± 0.98 、 53.34 ± 2.10 、 25.0 ± 12 、 -25.79 ± 4.91 。2018 年從金川泥炭地採集的 85 公分的岩心，在 0-1 公分處取 9 種不同植物樣本以及 35-36 公分處取 6 種不同植物樣本。同一層位的不同植物樣本的 ^{14}C 年齡可以相差幾百年。在表層的 9 種植物的 ^{14}C 年齡範圍從 -1332 ± 79 (現代) 到 140 ± 85 yr BP，而在 35-36 公分處 6 種植物的 ^{14}C 年齡範圍從 180 ± 74 yr BP 到 611 ± 106 yr BP。由此可見，泥炭 ^{14}C 定年並非很簡單，不同植物的 ^{13}C 值也變化很大，需要謹慎地對待泥炭定年和穩定同位素分析。本研究顯示，盡量不要選擇泥炭中 *Carex seed*、*Carex rhizome*、*Cyperaceae root*、*Carex angustior* Mac.、*Drosera rotundifolia* Linn.、*Potentilla fruticosa* L. 和 *Ericaceae branch* 等進行 ^{14}C 定年。同時，因為岩心取樣時，容易將較粗大的草、木本植物從上層插到下層，應避免選擇這樣的植物定年。另外在每 0.5 米的岩心段落應該取上、中、下三層樣本定年。

中文關鍵字：泥炭、植物種類、 ^{14}C 定年、 ^{13}C 、 C/N

Stable carbon isotopic analysis of riverine dissolved organic carbon by photochemical oxidation

Yu-Shih Lin¹、Jin-Jia Liang¹、George S. Burr²、Shing-Lin Wang²

(1)Department of Oceanography, National Sun Yat-sen University、(2)Department of Geoscience,
National Taiwan University

Rivers are a major transport pathway of terrigenous dissolved organic carbon (DOC). The stable carbon isotopes of DOC ($\delta^{13}\text{C}_{\text{DOC}}$) help to identify DOC sources and quantify their contribution. The analysis requires that DOC is quantitatively converted to CO_2 , a procedure prone to contamination. So far, such a technique has not been established in Taiwan. This study aims at developing an ultraviolet DOC oxidation method for freshwater samples. The experimental setup includes two ultraviolet light sources (one 500 W mercury lamp versus three 90 W UV-C lamps) and a vacuum extraction system. Results from the tests of experimental conditions show that the recoveries of DOC as CO_2 were comparable for both light sources, but varied with irradiation time, reaction temperature, and the headspace pressure of the reaction vessel and its connection with the vacuum system. Analysis of Gaoping River samples using the optimized method shows that the mean recovery of DOC was $95 \pm 12\%$ with a $\delta^{13}\text{C}_{\text{DOC}}$ uncertainty of 0.3‰ ($n=3$). The procedural blank was $24.5 \pm 3.5 \mu\text{g C}$ ($n=6$). The $\delta^{13}\text{C}$ values of water-soluble isotope standards treated with the method deviated from the certified values by $0.5\text{--}2.6\text{‰}$, a result attributed to background carbon in the Milli-Q water used to dissolve the standards. The method was used to analyze samples collected from four rivers (Zhoshui, Tsengwen, Laonung, and Gaoping Rivers). The $\delta^{13}\text{C}_{\text{DOC}}$ values (-33.1 to -24.7‰) were within the range of previously reported values for river DOC, supporting the applicability of this method in analyzing freshwater samples.

Keywords: riverine dissolved organic carbon, stable carbon isotopes, photochemical oxidation

Two-end-member mixing in the fluids emitted from mud volcano

Lei-Gong-Huo, Eastern Taiwan: Evidence from Sr isotopes

Hung-Chun Chao¹、Chen-Feng You²、Chun-Chang Huang¹

(1)Department of Earth and Environmental Sciences, National Chung-Cheng University、

(2)Department of Earth Sciences, National Cheng Kung University

Mud volcanoes are one of the most important conduits for deep seated materials to migrate upward in sedimentary basins, convergent margin, and subduction zones. Mud volcano Lei-Gong-Huo (MV LGH) is a unique mud volcano which is located on the mélange formation lying on the andesitic volcanic arc. Fluids emitted from 47 setalite mud volcanoes in MV LGH were sampled and measured their major, trace elements with $^{87}\text{Sr}/^{86}\text{Sr}$ ratios. Major elements of the fluids are Cl, Na, and Ca, which are distributed between 291 and 376 mM, 131 and 289 mM, and 48.9 and 313 mM, respectively. High content of B, Ba, Mn, and Sr with relative low concentration of S and alkalinity are also detected. Comparing with seawater, LGH fluids have lower Na/Cl, K/Cl, and Mg/Cl but higher Ca/Cl ratios, indicating water-rock interaction of igneous rock and paleo-seawater at source region. This interpretation has further supported by Sr isotopes, which show low value of $^{87}\text{Sr}/^{86}\text{Sr}$ ratio down to 0.70710. The result of spatial distribution showing strong negative correlation between Na, Ca concentration and Ca, $^{87}\text{Sr}/^{86}\text{Sr}$ ratios indicates two end-member mixing is the major chemical characteristic. The fluid interacts with igneous rock carrying high Ca, low Na and low $^{87}\text{Sr}/^{86}\text{Sr}$ ratio while those interact with sedimentary rock carrying low Ca, high Na and high $^{87}\text{Sr}/^{86}\text{Sr}$ ratio. The source from igneous region dominates eastern part of the mud volcanoes in LGH while sedimentary source dominates western part. Most mud volcanoes show mixing behavior between two sources. The most possible geological structure to perform the spatial distribution on the surface is the negative flower structure induced by a strike slip fault. In summary, fluids emitted from mud volcanoes in LGH are originated from two sources, which are water-rock interaction of paleoseater and igneous rock from the east and sedimentary rock from the west at depth, resulting from complex geologic background of mélange formation and migrating through the conduit provided by the fault.

Keywords: mud volcano, Mud volcano Lei-Gong-Huo, Sr isotopes

Zircon age and petrogenesis of the Telupid ophiolite in northwestern Sabah

Yu-Hsiang Chien¹、Kuo-Lung Wang²、Sun-Lin Chung²、Azman A. Ghani³、
Xian-Hua Li⁴、Yoshiyuki Iizuka⁵、Hao-Yang Lee⁵

(1)Department of Geosciences, National Taiwan University、(2)Institute of Earth Sciences, Academia Sinica, Taiwan; Department of Geosciences, National Taiwan University、(3)Department of Geology, Malaya of University、(4)State Key Laboratory of Lithospheric Evolution, Institute of Geology and Geophysics, Chinese Academy of Sciences, Beijing, China、(5)Institute of Earth Sciences, Academia Sinica, Taiwan

Sabah ophiolites generally include Banggi Island, Ranau, Telupid, and Darvel Bay ophiolites which are distributed from northwestern to southeastern Sabah. Previous studies suggest that Sabah ophiolites bear supra-subduction zone (SSZ) feature and formed during Late Triassic to Late Cretaceous, but their age and tectonic origin remain debated. This study presents zircon U-Pb dating and Hf isotope results and bulk-rock geochemical data of the Telupid ophiolite, to examine their origin for tectonic implications. The crustal section of the Telupid ophiolite is composed of basaltic andesites (SiO₂ up to 53 wt.%) and gabbros. The zircon U-Pb dating of gabbros show ages ranging from 47±2 to 42.5±0.3 Ma with positive ε_{Hf}(T) values from +22 to +16 for these zircons. Both basaltic andesites and gabbros display depleted light rare earth elements (LREE), nearly flat high rare earth elements (HREE), and their multi-element distribution patterns show depletion in high field strength elements (HFSE). In addition, their bulk-rock Sr-Nd isotopic compositions exhibit ε_{Nd}(T)= +9.4 ~ +8.8 and ⁸⁷Sr/⁸⁶Sr= 0.703024 ~0.703585. These data suggest that the Telupid ophiolite was a fragment of Eocene oceanic lithosphere generated in Mid-Ocean Ridge (MOR) setting. Since Eocene MOR-type ophiolite is discovered in Sabah, it indicates that not all Sabah ophiolites formed in SSZ setting during Mesozoic as previous thought. Furthermore, the Telupid ophiolite could associate with Eocene Palawan ophiolite (Hall, 2002) which is most likely to be a remnant of Proto South China Sea.

Keywords: Sabah, Eocene ophiolite, MOR-type

印尼爪哇西部新生代火山岩之年代學與地球化學特徵

梁瑋琪¹、賴昱銘¹、李皓揚²、辛怡儒³、Lediyantje lintjewas¹、
Iwan Setiawan⁴、Long-Xiang Quek¹

(1)臺灣師範大學地球科學系、(2)中央研究院地球科學系、(3)臺灣大學地質科學系、
(4)Research Center for Geotechnology, Indonesian Institute of Sciences (LIPI)

東南亞地區位於三大板塊，歐亞板塊、菲律賓板塊和印度—澳洲板塊聚集邊緣的交匯處，同時也包含了數個活躍的板塊隱沒帶，並有著許多由早期岡瓦納古大陸(Gondwana)分裂的地殼，歷經古生代至新生代的地質構造活動後聚集至現今東南亞位置。爪哇島位於巽他古陸(Sundaland)的南緣，為一平行於巽他-班達隱沒帶(Sunda-Banda Subduction Zone)之島嶼，依照大地構造的分布可分為西爪哇、中爪哇、東爪哇三個地塊。西爪哇以新生代火山島弧為主，其北部為巽他古陸大陸基盤，中、東爪哇以白堊紀增積的蛇綠岩體及島弧岩石為主，南部殘存的部分太古代大陸地殼則平行分布於爪哇全島。針對西爪哇研究的部分，前人在定年工作上有數個第三紀的鉀氬定年結果，並初步討論新生代火山在空間上的分佈；地球化學部分，前人工作僅有全岩主要元素的分析，因此本研究將於西爪哇地區採樣並進行了更詳細的定年與地球化學分析，從而試取得西爪哇地體演化架構相關線索，以及西爪哇各期火山活動之年代。

本研究於西爪哇採集了新生代之火山岩 (共 55 個)，並依照火山和地理位置把樣本分成五群(Danau 火山體、Bayah Dome 北部、Bayah Dome 南部、Gede 火山體、Ciemas 火山體)，進行鋁石鈾鉛定年分析與全岩地球化學分析。鋁石鈾鉛定年初步結果可將西爪哇的火山岩分兩期，分別為中期中新世(11~17 Ma)到晚期中新世(5.4~9.9 Ma)及更新世(小於 1 Ma)。空間上的分布：中期到晚期中新世出露在整個 Bayah Dome 地區(南、北部)；更新世火山岩為整個西爪哇最年輕的火山岩體，主要出露在 Danau 火山體、Bayah Dome 北部和 Ciemas 火山體；從初步結果可得知第三紀的岩漿活動具有由西爪哇南部向北部，呈現年代愈趨年輕的現象並呼應前人使用鉀氬定年結果之相同推論。另外，在 Bayah Dome 北部具有白堊紀年代約 140 Ma 之繼承鋁石紀錄，並可對比至蘇門答臘同時期的岩漿活動，顯示此岩漿活動由蘇門答臘南延至西爪哇北部。全岩地球化學中，主要元素指出此區域火山岩主要為鈣鹼質的玄武岩至石英安山岩 ($\text{SiO}_2 = 45\sim 69 \text{ wt.}\%$)；微量元素部分，輕稀土元素對重稀土元素有相對較富集的現象和微銷負異常，並且呈現高場強元素(high field strength elements, HFSEs) 虧損，特別是鈮、鉍及鈦(TNT)等元素，以及大離子親石元素(large ion lithophile elements, LILEs)富集，呈現典型的島弧岩漿地球化學特徵。

本研究發現印度—澳洲板塊在西爪哇地區呈現多階段的隱沒作用，並可將島弧火山的空間分布與噴發時間相聯結，地化部分還有待後續的全岩鋁鈹同位素與鋁石鈾同位素資料獲得後，做更進一步的岩石成因的探討。

中文關鍵字：印尼爪哇、巽他島弧、新生代火成岩、鋁石鈾鉛定年法、全岩地球化學



印尼西爪哇碎屑鋯石及繼承鋯石之鈾-鉛定年學研究

羅琳¹、賴昱銘¹、李皓揚²、辛怡儒³、Iwan setiawan⁴、
Lediyantje lintjewas¹、Andrie Al Kausar¹、Long Xiang Quek¹

(1)臺灣師範大學地球科學系、(2)中央研究院地球科學研究所、(3)臺灣大學地質科學系、

(4)Research center for geotechnology, Indonesian Institute of Sciences

爪哇島位於中生代巽他大陸核心的邊緣，是一平行隱沒帶之東西向島嶼。印澳板塊自中生代起開始向北漂移，並隱沒至歐亞板塊下方，形成多次的隱沒作用，期間也曾發生微板塊貼合事件，造成爪哇島由東向西之地體架構有所不同，依照其特徵可將爪哇島分為西爪哇、中爪哇和東爪哇。西爪哇北部的火成活動，為蘇門答臘向東延伸的白堊紀火山島弧，其他區域則以新生代火山島弧為主，火山活動年代包括第三紀及第四紀至今。前人針對西爪哇 Jatibarang 地層與南蘇門答臘出露之火成岩進行研究，發現兩者具有相似的岩性與特徵，但並未提出年代的證據。本研究於西爪哇採集砂岩（包括海砂），進行鋯石鈾-鉛定年分析，並搭配火成岩中分析所得的繼承鋯石，依據鋯石年代在時間與空間上的分布情形，試取得西爪哇在不同時期之鋯石來源區域，以及西爪哇各期火山活動之年代。

本研究共分析 5 個砂岩，分別採自 Ciemas 及 Cihara；以及 1 個位於 Bayah Dome 沿海的海砂樣本，總計 596 顆鋯石；並於 Danau 火山、Karang 火山及 Ciletuh 灣區採集的 3 個火成岩中，挑選繼承鋯石共 62 顆。目前年代分析結果指出：(1) 西爪哇西北部具有約 140 Ma 之鋯石紀錄，可與蘇門答臘同時期的岩漿活動年代做對比，此年代並未見於西爪哇南部樣本。(2) 西爪哇新生代以來之岩漿活動，具有遠離隱沒帶越趨年輕的現象，由南向北分別記錄到 25 Ma、17 Ma 及 11 Ma 三期事件。(3) 本研究於 Cihara 和 Bayah Dome 的砂岩及海砂中獲得始新世、白堊紀和三疊紀之碎屑鋯石訊號，結果顯示物源分別來自蘇門答臘、施瓦納山脈及錫帶花崗岩。

中文關鍵字：碎屑鋯石、鋯石鈾鉛定年學、西爪哇、巽他島弧、新生代岩漿活動

First report of ichnogenus *Phymatoderma* from Miocene Taliao Formation (NE Taiwan): Systematic ichnology, behavioral ecology and paleoenvironmental linkages

Wei-Lun Chen¹、Ludvig Löwemark¹

(1)Department of Geosciences, National Taiwan University

In the Northeast Coast of Taiwan, the ichnogenus *Phymatoderma* is first reported in the yellowish sandstone units of the Yehliu Member, Miocene Taliao Formation. In order to unravel its ichnological identity, ethology and its linkage to paleoenvironment, several different methods including overall observation (field and hand specimen), profile sectioning, thin section, micro-CT scanning and X-ray diffraction analysis are implemented. Interestingly, despite the trace being found within shoreface environment along with other *Skolithos* ichnofacies-trace fossils, the morphological analyses show that the trace fossil strongly resembles the ichnogenus *Phymatoderma*, which is previously considered to only appear in deeper marine environments (outer shelf/inner slope; *Zoophycus* ichnofacies). In terms of the ethology, some adaptations to the shoreface environment are presented, including densely packed pelletal active fillings and the lined wall in central shaft. Furthermore, the goethite which was found in the pelletal active fillings has implications for the possible diet of the trace maker. The result reveals not only the diversified ancient iconological activities but also the appearance of deep-sea trace fossil in shallow marine environment. Moreover, it implies that the appearance of *Phymatoderma* is not substantially controlled by the energy level, food resources, oxygen level and substrate stability behind the outer shelf/inner slope environment, but by other unknown environmental factors.

Keywords: *Phymatoderma*, northeast coast, Miocene Taliao Formation, shoreface, trace fossil, Taiwan

Stereomic microstructures of *Scaphechinus mirabilis* from Pleistocene strata in western Taiwan

Yu-Jou Lin¹、Jiamm-Neng Fang²、Jia-Kang Wang¹、Jih-Pai Lin¹

(1)Department of Geosciences, National Taiwan University、(2)Collection Management Department,
National Taiwan Museum

Problem: Stereomic microstructures known as stereom are the fundamental building blocks of echinoderm ossicles and they are key features to interpret the function(s) of echinoderm ossicles since Cambrian (~541 Ma). Stereom consists of three-dimensional mesh of trabeculae filled with interconnecting pores. Trabeculae is composed of high-magnesium calcite which behaves as a single crystal in each ossicle. Stereom studies are crucial to understand the phylogeny, growth and soft tissue of Echinoidea. Fossil echinoids from Taiwan have been studied for decades and many impressive collections are housed in both public and private museums in Taiwan, but no report of fossil stereom before.

Goal: The main purpose of this study is to document and report the fossil stereom preservation of a fossil clypeasteroid *Scaphechinus mirabilis* recovered from the Pleistocene strata in the western Taiwan. To understand better the stereom preservation of *S. mirabilis*, a total of 971 specimens deposited at the Department of Geosciences, National Taiwan University (NTUG) were examined. An additional 572 specimens were studied also.

Methods: Well-preserved specimens were prepared for thin sections, allowing interpretations of stereom types under polarized light microscope (PLM). Under PLM, echinoid ossicles boundaries can be recognized easily with open nicol and cross nicol settings. In order to enhance the contrast, an accessory plate (gypsum plate in this case) was inserted. Modern specimens of *S. mirabilis* from Japan were studied also under scanning electron microscope (SEM) for comparison.

Result: A total of 65 well-preserved fossil specimens and one modern sample were selected for making thin sections. Among the 86 thin sections, 68 sections were prepared and cut through the bilateral symmetry, and the other 18 thin sections were cut through different regions of the test, including apical system, petaloid, and interambulacral areas. Types of stereom and the associated tissues are determined by calculating the pore size and minimum thickness of trabeculae. Under SEM, tubercles of modern *S. mirabilis* can be subdivided into six regions. Our data show that plate boundaries, growth lines and stereom are clear and identifiable under PLM.

Remark: Dominant types of stereom include labyrinthic, rectilinear and galleried stereom. The average coarseness of tubercle boss is 10.9 μm , and the trabecular thickness is 12.3 μm . The porosity of tubercle boss is 0.89. The average coarseness of

tubercle areole is $18.6\ \mu\text{m}$, and the trabecular thickness is $10.2\ \mu\text{m}$. The porosity of tubercle areole is 1.8. On the oral-plate, some stronger radial trabecules penetrate into the adjacent plate in order to strengthen the connection in plates. The average trabecular thickness of this solid stereom spikes is $20.3\ \mu\text{m}$.

Keywords: Paleontology and stratigraphy, Stereom, Echinodermata, Sand dollars, Toukoshan Formation



Application of geometric morphometric methodologies to assess convergence in discoidal morphology in the sand dollar genera *Dendraster* and *Arachnoides* occurring from geographically isolated regions

Robert Swisher¹、Jih-Pai Lin¹

(1)Department of Geosciences, National Taiwan University

Clypeasteroids, sand dollars, have obtained a unique discoidal perimeter morphology along the curvature or ambitus. This distinctive flattened and rounded morphology appears adaptive to their shallow water life habitat, implying importance in the evolution of this trait. Currently, there is little understanding on how this morphology was obtained within some clypeasteroids. This study uses geometric morphometrics to examine fossil clypeasteroid specimens of *Dendraster ashleyi* from the western United States and compares with extant *Arachnoides placenta* material from Taiwan. The goals of this analysis are: 1) To quantify morphological, ontogenetic, and developmental variation for the examined clypeasteroid genera; 2) To quantify how discoidal morphology is developed in the examined genera; 3) To quantify lateral and posterior morphological variation for the examined genera; and 4) Examining how regional endemism and geographic isolation may effect morphological, developmental, and ontogenetic variation in Clypeasteroids.

This analysis forms the foundation for quantifying how this distinctive discoidal morphology evolved by assessing morphological variation and comparing developmental ontogeny between different clypeasteroids. Results demonstrate strong morphological variation and ontogenetic controls in the aboral/oral surfaces for ambitus and curvature change. Other examined morphologic features like the petaloid structures and the lateral and posterior profiles do not demonstrate apparent ontogenetic trends. Explanations for these trends includes interspecific variation or morphological variation controlled by environmental factors. Lastly, the results demonstrate the utility of geometric morphometric methods for assessing morphological and evolutionary questions within clypeasteroids. This work builds a foundation for broader study of the development of discoidal morphologies within clypeasteroids and their morphological and evolutionary history.

Keywords: *Clypeasteroida*, ontogeny, landmarks, Taiwan, paleobiogeography

Generic-level identification of *Astriclypeidae* based on onsite incomplete specimens from Yehliu Geopark, Taiwan

Ammu Sankar Senan¹、Robert Swisher¹、Jih-Pai Lin¹

(1)Department of Geosciences, National Taiwan University

Problem: Yehliu Geopark is famous with its Queen's Head made out of Miocene fossiliferous sandstone. Based on previous studies, there are two distinct forms of fossil echinoids with lunules: *Astriclypeus* sp. and *Echinodiscus* sp. Although they can be distinguished easily based on the number of lunules if complete, they are difficult to tell apart when they are disarticulate and fragmentary. In addition, fossils are located in national park, thus, all studies have to be done on site. Thus, it is hard to access the ecologic interaction between the two genera.

Goal: The main purpose of this study is developed a method to test if we can distinguish the two genera apart based on disarticulated specimens on site. The main advantage is that there are numerous specimens available to be tested and measurements with good statistical supports can be obtained.

Method: Landmark analysis is a great tool that can be used to understand the variations in different organismal factors based on morphology. Hence, it can reveal information about the evolutionary and biological processes as well as the morphological deviations. The first attempt is to take capture good digital images with scales, then perform landmark analyses with them afterward.

Result: Three and seven landmark points were taken from each specimen image. A total of 55 specimens, including both *Astriclypeus* and *Echinodiscus* genera, were examined for the study. The results of the three landmark point data set reveal generic level distinct clustering of data during the principal component analysis (PCA) for the two possible genera present, which are *Astriclypeus* and *Echinodiscus* of the *Astriclypeidae* family. A much similar trend with distinct clusters for the two different genera was displayed even in the results of the seven landmark point data set.

Remark: This study shows that the landmark analysis can be used efficiently for a generic level identification despite the specimen incompleteness, and the minimum number of landmark points. Hence this analysis could also be applicable for broader population studies in more likely settings. In addition, ratio measurements with a digital calibrator were made and will be analysed with PCA method for comparison.

Keywords: paleontology and stratigraphy, *Echinodermata*, *Echinoidea*, *Astriclypeidae*, landmark analysis, PCA

臺南曾文溪剖面六重溪層的沉積環境及其構造意義

莊釗鳴¹、洪崇勝²、謝凱旋¹

(1)經濟部中央地質調查所、(2)中央研究院地球科學研究所

臺灣位於歐亞大陸板塊與菲律賓海板塊交界處，碰撞造山使得臺灣島生成，並在造山帶西緣形成前陸盆地，而隨著造山帶持續向西演進，早先堆積在盆地中的沉積物便被擠壓與抬升。為了解前述自盆地下陷堆積與擠壓抬升的過程，本年度的自行研究選定臺南曾文溪烏山頭斷層下盤的澧水溪層、六重溪層與崁下寮層進行調查，期望藉由沉積相分析與磁生物地層資料，建置高解析的沉積地層柱以作為區域性對比的基礎，其中六重溪層可依沉積循環的特徵區分為六重溪層下段與上段。沉積相分析顯示澧水溪層、六重溪層及崁下寮層為一淺海大陸棚的沉積環境，可再次分出遠濱相、遠濱過渡帶相、濱面相、下蝕水道相以及海底峽谷相等 5 個沉積相。綜觀沉積相的垂直變化，指示澧水溪層由遠濱變淺至遠濱過渡帶相，六重溪層下段由遠濱與下蝕水道相向上變淺，轉以遠濱過渡帶與濱面相為主的上段。六重溪層上段由遠濱過渡帶至濱面相組成，上部被海底峽谷截切，並堆積海底峽谷相及其上覆的遠濱相沉積物。六重溪層的沉積循環週期約為 2.6-3.7 萬年，較此時期以 4.1 萬年週期主導的米蘭科維奇循環短，我們認為這可能與前陸盆地下陷或氣候循環之週期改變有關。

中文關鍵字：六重溪層、前陸盆地、烏山頭斷層、沉積環境

滄海桑田話南科

楊小青¹、Mayaw-Kilang¹、陳文山²

(1)國立臺灣史前文化博物館南科考古館、(2)臺灣大學地質科學系

國立臺灣史前文化博物館南科考古館為了配合南部科學園區成長管理及科技產業發展，評估台南園區未來發展擴建之可行性，依據文化資產保存法第 58 條規定，就目前評估擴建範圍進行地質土層調查，了解該區域有無相關考古遺址及文化歷史內涵，以作為園區發展擴建或籌設之參考依據及重要評估指標。因此受託在看西農場進行地質鑽探研究，除了了解是否地下保存史前文化相關文資或界定史前遺址的範圍，亦可藉鑽探土芯的研究重建看西農場的古環境變遷。本計畫共進行 100 孔岩芯鑽探，每孔深度 20 公尺，除了確認岩芯是否含有文物遺留進行文化遺址調查之外，也利用岩芯進行詳細的岩芯紀錄以及碳十四定年，配合全區已完成調查與發掘之史前遺址位置及文化內涵，探討南科地區 6 千年來古海岸變遷及其對史前文化人土地利用之影響。

中文關鍵字：古環境重建、考古遺址、南科園區



千年以來南海的巨波浪事件：澎湖海岸的地層記錄之三

游能悌¹、呂政豪²、顏君毅³、顏一勤⁴

(1)清華大學通識中心、(2)澎湖科技大學觀光休閒系、(3)東華大學自然資源與環境學系、
(4)中央大學應用地質研究所

台灣海峽經常受到颱風與海嘯津波等巨波浪事件侵襲，但是缺乏足夠的歷史事件紀錄與災害描述，仍然難以有效評估溢淹規模與再發生間隔。有鑒於此，選取面向馬尼拉隱沒帶與南中國海的台灣海峽南部海岸，包括澎湖諸島與嘉南海岸平原，進行上部全新統海相事件地層學與沈積學的調查與分析，在本年度（三年期程第三年）已經首先完成中屯嶼、白沙嶼、西嶼的海岸露頭調查，並發現十一個含有海相事件堆積層的剖面。

在中屯嶼四個剖面共發現三層海相事件礫石層，白沙嶼六個剖面共發現五層海相事件礫石層，西嶼東南邊牛心山一個剖面發現一層海相事件礫石層。這些事件層多具有侵蝕底面、海相化石碎屑、圓形岩礫等特徵，並可分為二大類。一類事件層的高程都在 2 公尺以上，遠高於颱風暴潮水位，基質支持反映高濃度沈積物碎屑流的堆積作用，可能與海嘯作用比較相關，碳十四定年結果中，年代指向五個區間：五一六世紀、晚十三世紀、十五—十六世紀、十七—十八世紀、與二十世紀。另一類高程都在 2 公尺左右，接近於颱風暴潮水位，顆粒支持、具有層理，反映高濃度沈積物拖曳流的堆積作用，可能與颱風暴潮作用比較相關，碳十四年代指向二個區間：從十八—十九世紀、現代。

第一類疑似古海嘯堆積層可以比對前二年的研究成果，第二類疑似古颱風堆積層，也可以比對前二年的研究成果，呼應歷史與現代颱風的紀錄，包括澎湖廳志與中央氣象局。

中文關鍵字：颱風暴潮、海嘯、海相事件堆積層、上部全新統、中屯、白沙，
西嶼

Machine learning for facies classification: a new approach based on high-resolution element data from shallow marine sediment cores (East Frisian Wadden Sea, Germany)

An-Sheng Lee¹、Dirk Enters²、Bernd Zolitschka³、Sofia Ya-Hsuan Liou⁴

(1)National Taiwan University, Department of Geosciences and Research Center for Future Earth, Taipei, Taiwan; University of Bremen, Institute of Geography, Germany、(2)Lower Saxony Institute for Historical Coastal Research, Wilhelmshaven, Germany、(3)University of Bremen, Institute of Geography, Germany、(4)Department of Geosciences, National Taiwan University

Sediment facies classification is an important first step to investigate depositional environments and provides primary information for further analyses and interpretations. The conventional method relies on sedimentological observations and experience, which include a macroscopical description of color and sediment structure, basic chemical and physical tests, and the evaluation of biological remains. Without time- and labor-consuming quantitative measurements, these classifications are not objective and not easy to re-evaluate. We propose high-resolution core scanning as an alternative of human observation and an automatic facies classification model that was trained by a subset of conventionally identified facies to minimize the disadvantages of standard core descriptions and facies classification. For this study, we make use of 92 sediment cores that have been retrieved from the coastal area around the island of Norderney, Germany. These sediments were classified by a group of sedimentologists into 12 facies, including marine (e.g. shoreface, channel and sand flat sediments) and terrestrial (e.g. peat and moraine deposit) sediments. Our approach is based on 2 mm resolution profiles of 12 elements from these sediment cores, acquired from an Itrax X-ray fluorescence (XRF) core scanner. These measurements are expected to correspond with human observations. Machine learning algorithms (Logistic regression, Random forest and Support vector machine) have been applied and cross-validation was used to determine the optimal model. The performance of the best model reaches 61% prediction accuracy in a test set, which is promising compared to a random guess from the same 12 facies. Two matrices (confusion matrix and conjunction matrix) are provided to understand the performance in more detail. Our result is a further step to introduce machine learning techniques into the field of geosciences and gives a broader coverage of sediment in diversity and quantity.

Keywords: sediment facies classification, Wadden Sea, μ -XRF core scanning, machine learning

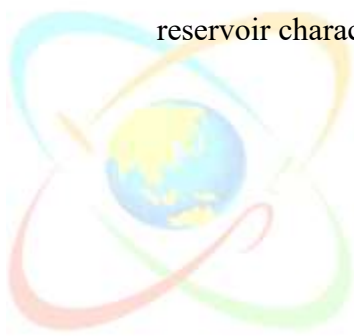
Petrel Reservoir Modeling – Integrated workflow on geothermal reservoir characterization

Andy Min-Hao Wang¹

(1)Schlumberger

The Petrel E&P software platform is the standard tool in the oil and gas industry, it brings various disciplines together, such as geosciences, reservoir engineering, production engineering, and drilling. This shared earth approach enables companies to standardize workflows from exploration to production, so they can make better decisions based on a clear understanding of both opportunities and risks. In the presentation, we are applying the integrated workflow from oil and gas to geothermal reservoir characterization. In the proposed workflow using Petrel, it allows the combination of all the geological and geophysical data to characterize the geothermal reservoir and create a 3D model to visualize all features of the hot water system.

Keywords: Petrel E&P software platform; 3D reservoir modeling; geothermal reservoir characterization



Wireline openhole logging for geothermal reservoir

Ching-An Lee¹

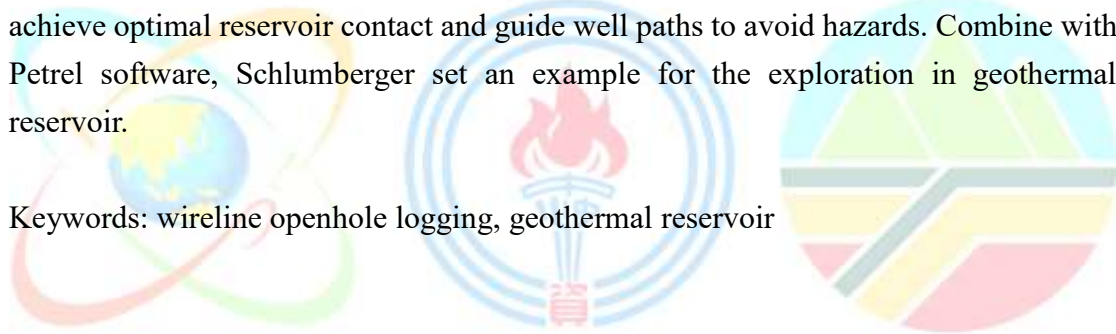
(1) Schlumberger Overseas S. A.

Schlumberger provide the advanced technology to reveal the geologic details in oil and gas industry. Wireline openhole logging deploying sensors to measure all aspects of the reservoir in real time. CPC Corporation, Taiwan adopted our wireline logging services into geothermal reservoir from 2018 to 2020.

We had provided several openhole logging services in geothermal reservoir. From PEX-HRLA-DSLIT (triple-combo neutron, density, resistivity and slowness), FMI (Fullbore formation microimager), DSI (Dipole Shear Sonic Imager) to MAST (Multimode Array Sonic Tool, Sonic Scanner).

In the presentation, we are demonstrating the various data we acquired from wireline openhole logging in the reservoir. We provide the answers for informed decision making and risk reduction from precise and accurate downhole logging measurements. Understanding local and field-wide structure and variability helps to achieve optimal reservoir contact and guide well paths to avoid hazards. Combine with Petrel software, Schlumberger set an example for the exploration in geothermal reservoir.

Keywords: wireline openhole logging, geothermal reservoir



The magnetic inversion by using the velocity-based initial model

Chun-Rong Chen¹、Jann-Yenq Liu²

(1)Industrial Technology Research Institute; Department of Space Science and Engineering, National Central University、(2)Department of Space Science and Engineering, National Central University

Non-uniqueness is a problem encountered while imaging subsurface susceptibility by inverting magnetic field surveys. We propose a novel method to construct velocity-susceptibility initial models using V_p together with the V_p/V_s ratio from seismic tomography to improve the model which satisfies more information and better identifies locations of high-susceptibility materials. For comparison, two recovered susceptibility structures are derived from two distinct initials (homogeneous and velocity-susceptibility) models through the standard inversion process. Two profiles with the intense undulation of magnetic anomalies over sedimentary areas in central-west Taiwan and complex geological structures at the rim of the subduction zone in northeast Taiwan are used as examples to compare the results of the initial models. The inversion results suggest that the susceptibility structures from both models agree in terms of the location of the fault zones, specifically at depth < 10 km. Recovered susceptibility structures derived from the velocity-susceptibility initial model agree with the geological structure that reduces uncertainty at depth > 10 km. Consequently, the initial model with velocity constraints lowers the non-uniqueness associated with the inversion of magnetic anomalies.

Keywords: magnetic anomaly, geothermal energy, velocity tomography

A role of geothermal heat on energy conservation: Implications for Green (low-carbon) campus in Taiwan

Sheng-Rong Song¹、Yi-Chia Lu¹、Chyi Wang¹

(1)Department of Geosciences, National Taiwan University

Energy policy includes production, conservation and storage, which the geothermal heat can play all of the roles. For example, the geothermal heats can construct a power plant for electricity supply, to build up heat pump for district heating and cooling on saving energy, and to store the energy underground for future utilization. The direct utilization of shallower geothermal energy, the heat pump is the most widely uses in the world, which may be up to over 70.32 GWt currently. It can be applied on district heating in high latitude, and on local cooling in low latitude. Based on the cooling experiments of heat pumps in tropical and subtropical countries, i.e. Vietnam, Thailand and Indonesia etc., the energy conservation of those testing can save the power up to 50%. Therefore, the International Energy Agency (IEA)-Geothermal promotes the direct uses of geothermal heat in last decade in the world. Taiwan is located in tropical and subtropical areas, which the average season temperatures are 28°C and 16°C in summer and winter, respectively. Based on the statistics of Taipower, the summer need more about 2.2 billion KWh extra-electricity monthly for cooling than winter. Meanwhile, the cooling system uses air as media and discharge heat out to street to induce the temperature up and phenomena of heat island in most Taiwan metropolitan cities. Moreover, the Executive Yuan announced to install air conditioners for all of the elemental and high schools in Taiwan that will increase the usages of electricity and power structures in the future. The heat pump for cooling may provide a solution for not only to save energy and reduce the electricity shortage, but also lower temperature and heat island of a city in Taiwan. Furthermore, the heat pump can also play a role on green (low carbon) campus of university or industrial parks, which is the world trend for reducing carbon emissions.

Keywords: geothermal energy, heat pump, Green campus, Taiwan

三維離散裂隙網路模擬－以大屯火山區為例

黃淞洋¹、林朝彥¹、葉恩肇²、鍾權偉¹、溫心怡¹、陳棋炫³、林昶成³

(1)工業技術研究院材料與化工研究所、(2)臺灣師範大學地球科學系、(3)經濟部中央地質調查所

地熱潛勢區的熱水儲集層大多為高孔隙率或是裂隙發達的岩層，上方則有能封存熱能的緻密岩體做為蓋層，熱水或高溫蒸氣往往經由斷層及裂隙通道進行傳輸遷移，當熱水(氣)傳遞至地表則成為地熱徵兆區；因此，如何透過地表及井下裂隙分布等有限的資訊，推測大範圍地下裂隙空間分布，作為後續地熱概念模式建置及潛能開發評估的參考，是地熱探勘的關鍵性工作之一。

離散裂隙網路(Discrete Fracture Network, DFN)模擬係針對特定空間範圍內，藉由統計方法分析地表及井下裂隙的參數特性，建立三維裂隙網路的空間分布。DFN 模型除了可滿足現地露頭及井下的裂隙特徵之外，更可將裂隙空間分布擴大至尚未進行鑽井的區域，亦可藉由剔除不連通的裂隙，僅就連通至地表的裂隙群及現有調查結果所推測的地下水流連通構造(如正斷層系統等)進行分析，對比於地表地下水出露位置或是地熱徵兆區，評估熱流可能的傳輸路徑。

大屯山地區共完成 12 處地表裂隙參數量測，並繪製相對應的位態極點投影圖及裂隙軌跡分布圖，其中裂隙位態經 K-S 檢定後均可使用費雪分布描述，地表露頭及井下分析的裂隙強度則可藉由理論方法的計算方式，將裂隙線強度及裂隙面強度轉換為裂隙體密度，並可藉由分析地表裂隙軌跡長度及大尺度地表線型判識成果，分析大屯火山區裂隙尺寸的冪方律函數。依照現有的裂隙軌跡長度計算的冪方律指數及相對應的裂隙位態、裂隙強度，分別建立磺嘴山及大磺嘴地區的 DFN 模型，模擬結果說明研究區域內主要仍為斷層或是其它大型導水構造主導地下水及熱流傳輸，裂隙面則代表除了主要通道之外連結至地表的次要通道，出露地表可能形成地熱徵兆區或是降水入滲的區域。

中文關鍵字：離散裂隙網路、裂隙參數、冪方律函數

**Influences of stress variation on the evolution of 3D fracture system:
An example in NE Taiwan**

En-Chao Yeh¹、Huong-Thi Pham¹、Ping-Chuan Chen²、Yu-Chang Chan³、
Chih-Hsiang Yeh⁴、Kuo-Jen Chang⁵、Yu-Chung Hsieh⁶

(1)Department of Earth Sciences, National Taiwan Normal University、(2)Department of Geosciences, National Taiwan University、(3)Institute of Earth Sciences, Academia Sinica, Taiwan、(4)Department of Civil Engineering, National Central University、(5)Department of Civil Engineering, National Taipei University of Technology、(6)Central Geological Survey, MOEA, Taiwan

Fractures can be nucleated and/or reactivated by appropriated stress state. It is well established that NE Taiwan has been experienced the tectonic evolution from oblique collision to backarc extension in the view of stress variation during late Cenozoic. In this study, we will verify whether fractures in NE Taiwan can be manipulated by the stress change along the NE coastline of Taiwan.

3D fracture maps and stress state are two essential elements in this experiment. We recognized 120 of 187 reliable fractures based on DEM analysis and interpretation and further calculated their attitudes. Stress inversion was conducted from focal mechanism data of 1991 to 2016. Inferred stress state can be divided into 3 domains with 12 cells from north to south. After evaluating the fracture instabilities with corresponded stress path, it is realized that surface fractures in DEM could be nucleated with the applied stress field in the evolution of the tectonic setting from the south to the north along the coastline area at NE Taiwan. We also examined the slip tendency to explore the reactivation tendency of nucleated surface fractures. The results confirmed the important role of the back-arc extension of Okinawa Trough opening to reactivate surface fractures in NE Taiwan. Therefore, correlation between 3D fracture map and stress state can afford vital applications in terms of the landslide, groundwater, site characteristics and scientific research issues.

Keywords: fracture instability, 3D fracture system, stress, NE Taiwan

The remaining exploration potential of onshore Taiwan as evidenced by the evolution of oil and gas discoveries in the Llanos basin, Colombia

Duen-Chien Mou¹、Ruei-Tze Huang¹

(1)Formosa Energy Co., Ltd.

Onshore Taiwan exploration had enjoyed some major successes in the Chu-Miao area in the 1960s and early 1970s by exploiting deeper reservoir targets and drilling prominent anticlines defined mainly by surface mapping. This high degree of success began tapering off after the late 1970s, with just a few smaller fault trap and biogenic gas discoveries made south of the Peikang High. On the other hand, Llanos basin has been the most important oil producing basin in Colombia for decades where new discoveries have been made continuously since the 1960s.

When comparing exploration history of onshore Taiwan to the Llanos basin, one can notice that both places had started their exploration effort in a similar humble fashion. Subsequent development of new exploration concepts and implementation of modern technologies in the Llanos basin by various oil companies, however, have not progressed satisfactorily in Taiwan.

With further application of 3D seismic, depth imaging, dynamic petroleum system modeling, reservoir facies analysis, and directional and horizontal drilling, most of the successful plays in Llanos like sub-thrust duplex structures, subtle fault and stratigraphic traps, downthrown fault closures, can have good chance to be duplicated in Taiwan. Adding turbidite channel-fan and mud diapir plays existing in southern Taiwan but not in Llanos, exploring onshore Taiwan by testing high-potential but low-risk prospects is expected to produce significant amount of new hydrocarbon reserves.

Keywords: exploration history, exploration potential, Llanos basin, onshore Taiwan

中東碳酸鹽岩礦區封閉構造研究

李健平¹、蘇俊陽¹、張國雄¹、廖韡智¹

(1)臺灣中油公司探採研究所

碳酸鹽岩儲集層在全世界的產油氣量佔 60%以上，本公司過去多著重於碎屑岩沈積環境的油氣探勘，對碳酸鹽岩石油系統與油氣探勘均缺乏相關經驗。因此，本研究計畫針對中東碳酸鹽岩礦區進行研究，分析礦區內二維與三維震測資料，並搭配井測資料，嘗試找出研究區域具有油氣潛能之封閉構造。期望藉由分析實際碳酸鹽岩礦區資料，增進碳酸鹽岩類型油氣探勘經驗。本研究先利用井測資料計算的合成震波與震測資料進行比對，找出目標地層在震測剖面所對應的訊號，藉以延伸解釋目標地層頂部構造圖。由震測剖面可知，震波訊號有明顯的側向變化，應是此區域存在許多小型礁體所造成。根據 K、M 和 B 三個三維測區與礦區東部二維測線之震測解釋結果，確認 K 測區之淺部地層有 2 個封閉，分別為背斜構造形成之四方圈合封閉與地層尖滅封閉；M 測區之深部地層有 2 個封閉，分別為深部斷層封閉及淺部背斜構造形成之四方圈合封閉；B 測區之深部地層有 3 個背斜構造形成之四方圈合封閉；礦區東部二維測線的淺部有 1 個背斜構造。除此之外，本研究也針對深部構造結合屬性分析，找出 3 個可能探勘標的。本研究分析的碳酸鹽岩封閉構造類型，可提供做為未來探勘之參考。

中文關鍵字：碳酸鹽岩、震測解釋、四方圈合、斷層封閉

多元測繪技術於山區公路易致災邊坡應用 - 以臺 20 線

178K+450~178K+819 路段為例

王貽德¹、何岱杰²、許書凱³、黃貞凱³、林志交⁴、林慶偉¹

(1)成功大學地球科學系、(2)臺灣電力股份有限公司、(3)黎明工程顧問有限公司、

(4)中興測量有限公司

近年來受氣候異常影響，強降雨頻率增高，南橫公路崩塌頻傳且規模漸趨擴大。而山區公路因常伴峽谷及溪流而行，邊坡陡峭人力不易抵達，故巡檢視角有限。若無法精確的獲取邊坡環境調查資訊，即無法有效的瞭解崩塌災害成因與風險，協助崩塌風險分級及管理，進而降低崩塌災害發生機率。

本文針對南橫公路 178K+450~178K+819 路段，藉由包含 UAV/UAS(無人飛行載具)、LiDAR(地面光達掃瞄)及大尺度 LiDAR(空載光達掃瞄)等多元尺度測繪技術設備，獲取高解析度地形樣貌與產製高精度三維數值地表模型。同時蒐集近五年高解析度衛星或航空影像圖資，準確掌握區域地形構造位置與變化範圍，並輔以 Coltop3D 軟體進行不連續面位態分析，進而評估該易致災邊坡路段崩塌風險分級及提出改善方案建議。

中文關鍵字：多元尺度測繪技術、無人飛行載具、光達掃瞄



台灣斷層破裂至地表機率模型之建置

張志偉¹、張毓文¹、趙書賢¹

(1)國家地震工程研究中心

當中大規模的極淺地震發生時，其所引致之地表破裂將造成地上建物或橋梁損壞，例如 1999 年集集地震及 2018 年花蓮地震，部分橋樑及建物均因地表錯動而造成嚴重損傷。有鑒於此，錯動量是為耐震設計重要參考。因地震引致之錯動量，除以經驗式直接進行估算外，亦可採用機率式斷層錯動量危害分析 (Probabilistic Fault Displacement Hazard Analysis, PFDHA)。在進行機率式分析時，須了解地震發生時是否引致地表破裂，機率為何，以評估鄰近斷層之工址，在特定的地震回歸期中，計算可能的地表斷層錯動量，做為日後重要設施地震影響之評估。本研究將應用台灣歷史地震紀錄，發展斷層破裂至地表機率模型，提供機率式分析之參考。

利用中央氣象局於 1900 年以來規模 5.0 以上、深度小於 20 公里之地震目錄，以及 Taiwan Earthquake Model 於 2015 年所公布台灣陸上 38 條活動斷層之位置，利用震央分佈與斷層跡線之相對位置，將台灣陸上可能與斷層活動有關的地震事件篩選出。除此外，本研究蒐集中央氣象局 1901-2000 年的災害性地震列表 91 筆地震事件(<https://scweb.cwb.gov.tw/zh-tw/page/disaster/5>)、台灣十大地震災害地震圖集、中央地質調查所特刊與其他文獻資料，依其對於地震災害的文字描述與災情嚴重程度，篩選因斷層錯動而造成地表破裂的地震事件。綜合上述兩組地震資料庫，區分出屬於斷層地震且有破裂至地表以及未破裂至地表之事件，再利用「邏輯迴歸模型」(Logistic Regression Model)(Hosmer and Lemeshow, 1989)建置屬於台灣本土陸上斷層破裂至地表的機率模型，此機率模型會與震源相關參數有關，如地震規模、震源深度與震源機制解等。地震規模越大、震源深度越淺，則代表斷層破裂至地表的機率越大。

本研究建立與地震規模有關的破裂機率模型，且不對各事件進行震源機制解的分類，將陸上所有斷層與所有地震事件視為一體。機率模型所得到的初步成果為：若台灣地區陸上發生一顆規模 6.5 且深度小於 20 公里的地震，其斷層破裂至地表的機率為 37.3%；若規模 7.0 且深度小於 20 公里的地震，其斷層破裂至地表的機率則為 74.0%。

中文關鍵字：邏輯迴歸模型、條件機率模型

深開挖基礎與上覆土層受正斷層錯動之影響

方儒雅¹、林承翰¹、林銘郎¹

(1)臺灣大學土木工程學系

近年的地震事件顯示除了強地動之外，斷層錯動造成的同震地表變形也是斷層附近結構物產生破壞的原因。台灣人口稠密，建物用地無可避免的會與斷層帶有交集，例如屬正斷層的山腳斷層鄰近台北盆地，斷層帶上有許多高樓結構物使用筏式基礎搭配連續壁(即深開挖基礎)，連續壁向下延伸增加了土層與基礎互制行為的複雜性，此複雜性又進一步加深了量化評估筏式深基礎與上覆土層受正斷層錯動之影響的難度。

為有效降低斷層錯動可能形成的災損，本研究使用基於有限差分法耦合離散元素法的三維數值模型，離散元素法模擬受正斷層錯動下產生應變集中帶的上覆砂土層，有限差分法則模擬筏式基礎結構物因斷層錯動和地表變形產生的反應。為了確認此耦合分析方法能合理模擬上述複雜課題，本研究建立三個基本案例模擬與理論解比較，也進行一系列的縮尺砂箱實驗與數值模擬結果相互校核，最後透過真實案例模擬來確認分析方法能合理地應用於全尺度現地案例。

基礎中心與斷層尖端之相對位置為本研究之主要變因，結果顯示位在斷層尖端上方的基礎由於為三角剪切帶所包圍，會產生明顯的位移並傾斜，斷層影響範圍增加並在兩側出現主、被動破壞；當基礎與斷層尖端保持適當距離時，基礎則沒有明顯變形且可有效阻擋三角剪切帶發育。根據當前研究城成果，本研究建議在設計結構物配置時若無法保持距離，靠上盤側配置能受較少影響，並採取適當調適措施，減少其受地表變形之損害。

中文關鍵字：正斷層、同震地表變形、土壤與基礎互制、深開挖基礎、耦合有限差分法與離散元素法

Multiple-segment rupture and earthquake probability in fault system

Chung-Han Chan¹

(1)Earthquake-Disaster and Risk Evaluation and Management (E-DREaM) Center, National Central University; Department of Earth Sciences, National Central University

Several seismic events are attributed to ruptures on multiple seismogenic structures during coseismic periods. Their instantaneous ruptures along large structures patches generate earthquakes with large magnitudes, resulting in fatality and damage. Thus, this study aims to understand interaction between seismogenic structures through identifying potential structures that could rupture instantaneously in a coseismic period and assessing seismic hazard. For such purpose, triggering interactions between seismogenic structures will be discussed through the Coulomb stress model; earthquake probability will be quantified using both statistics- and physics-based approaches through the Gutenberg-Richter relationship and the rate-and-state friction model, respectively. In order to evaluate their credibility, these models will be applied in the earthquake cases, including the 1935 Hsinchu-Taichung earthquake. Based on the multiple-structure system database summarized through this proposal and distribution of recent earthquakes, dynamic seismic hazard map platform that could be revised in real time will be proposed, beneficial to both subsequent researches and promotion of popular science.

Keywords: Earthquake probability, seismic hazard assessment, Coulomb stress change, Gutenberg-Richter law, rate-and-state friction law, scaling law

Characteristics of earthquake source and ground motions in northern Vietnam investigated by the 2020 Moc Chau M5.0 earthquake sequence

Nguyen Cong Nghia¹、Van Duong Nguyen²、Le Minh Nguyen³、
Van Bang Phung⁴、Bor-Shouh Huang⁴、Anh Duong Nguyen³、
Quang Khoi Le³、Thi Giang Ha³、Dinh Quoc Van³、Ha Vinh Long⁵

(1)Taiwan International Graduate Program Earth Sciences System, Academia Sinica, Taiwan、

(2)Institute of Geophysics, Vietnam Academy of Science and Technology, Vietnam; Graduate University of Science and Technology (GUST), Vietnam Academy of Science and Technology、

(3)Institute of Geophysics, Vietnam Academy of Science and Technology, Vietnam、(4)Institute of Earth Sciences, Academia Sinica, Taiwan、(5)Taiwan International Graduate Program Earth Sciences System (TIGP-ESS), Academia Sinica, Taiwan; Institute of Geophysics, Vietnam Academy of Science and Technology, Vietnam

On July 27th, 2020, a magnitude (Mw) 5.0 shallow earthquake occurred near Moc Chau, northwestern Vietnam. Several shallow aftershocks followed the mainshock and clustered in a small area. The mainshock caused damage to infrastructures in the source area. Significant shakings were felt at many new high buildings in surrounding cities. The ground motions of the mainshock and its aftershocks were well recorded by the national seismic network of Vietnam to analyze this earthquake sequence. The focal mechanisms of these events showed their major contribution from strike-slip movements. After this earthquake, a field survey has been carried by the research team of the Institute of Geophysics, Vietnam Academy of Science and Technology, Vietnam. A combination of damages pattern and source mechanism from moment tensor inversion analysis reveals this earthquake sequence might be associated with the active right-lateral Da River fault. The new archived seismic observations of this earthquake sequence have been analyzed to evaluate characteristics of earthquake source and seismic wave propagation in northwestern Vietnam and to discuss its potential earthquake engineering applications in northwestern Vietnam.

Keywords: Moc Chau earthquake, focal mechanisms, strike-slip fault, ground motion

假戲真做古海嘯

齊士崢¹、施雅軒¹、顏君毅²、陳佳宏¹

(1)高雄師範大學地理學系、(2)東華大學自然資源與環境學系

學者依據「臺灣采訪冊」「祥異」記載的「加藤港暴漲」，及相關數學模式模擬，認為南部地區可能發生 5 公尺以上的海嘯。「加藤港暴漲」發生於乾隆 46 年 (1781)，是由嘉慶元年 (1796) 錄取的恩貢生林師聖於道光 10 年 2 月 20 日 (1830) 所報。傳世的「臺灣采訪冊」是傳抄本，原始版本已經亡佚。林師聖是臺灣縣人，雖生卒時間不明，但仍可推測災害事發 49 年後才經採訪、記錄，而沒有發生當時官方記錄的「加藤港暴漲」事件，極有可能發生於他的幼年時期之前，而他後來是聽聞自當事人、目擊者，或是輾轉聽聞的鄉野奇譚，均未說明。不過可以確定的是乾隆 46 年時高雄、屏東平原已經納入清帝國鳳山縣治理，加藤港始終屬於「港東里」，直至日治時期亦從未劃分於「港西里」，當然更跟「鳳港」或「西里」無關。再由文獻與古地圖資料分析，「加藤港」是河口港，位於現在的東港、林邊之間，乾隆年間是港東里的重要港口，所以「港有船通郡」。不過「加藤港」至道光年間因河川改道、港灣淤積而消失了。至於「加藤港暴漲」記載的「水漲數十丈」，若非筆誤就是指稱水平距離，絕非高度。會被認為是兩波波高分別是 3 至 5 公尺海嘯，則是學者對於報導中「嗣聞是日」發生的另一個現象的一廂情願詮釋。以當代對海嘯破壞力的理解，人攀援木竹、茅草屋頂而至尾，或在搖曳的竹上避難，應該沒有機會在 3 至 5 公尺的海嘯中全體存活。「加藤港暴漲」的疑點實在太多，因嚴重的災害而喪命的竟然是一位「不孝悍婦」，能夠被傳說、記錄，不可忽視的重要原因恐是緣於其規訓婦女的隱喻意義。謠言現象不是今日才有，脫離現實的記載早應該認定為不實傳言的假新聞而以結案處理，實在無需如此費盡心思地牽強附會、擴大恐懼。不過「加藤港暴漲」是海嘯的真偽與高屏海岸是否曾經發生海嘯純屬不同議題，全世界的海岸也當然都有面臨海嘯災害的可能性，但「可能性」與「事實」不同，「面臨海嘯災害」不應該是問題的核心，「可能性」或者「風險」才是重點。高屏海岸是否有古海嘯地質記錄和未來面臨的「海嘯風險」，是更需要進一步研究和確認的主題。

中文關鍵字：臺灣采訪冊、加藤港暴漲、古海嘯、風險

The role of fluid drainage in fault slip zone during earthquake propagation

Nguyen Thi Trinh¹、Li-Wei Kuo²

(1)Department of Earth Sciences, National Central University、(2)Department of Earth Sciences, National Central University; Earthquake-Disaster and Risk Evaluation and Management (E-DREaM) Center, National Central University

Clay gouge is a common material in the brittle fault slip zone. Because of its low frictional strength, clay gouge plays as an important role in controlling the frictional strength of slip zone during the movement, e.g., earthquake propagation or landslides. The host rock adjacent to the slip zone can be either conduit or barrier for fluid flow during fault movement, yet the effect of fluid drainage on fault strength (behavior) is still poorly understood. To understand the effect of fluid drainage on the frictional strength of slip zone, we conducted rotary shear rock friction experiments on water-saturated kaolinite gouge under undrained and drained conditions. In addition, we use two kinds of filter paper to simulate different efficiency of fluid drainage under drained conditions. All experiments we conducted at a normal stress of 10 MPa and a slip rate of 1 m/s with total displacement $\sim 5\text{--}7$ m. The results show that (1) under undrained conditions, the friction coefficient (the ratio of shear stress/normal stress) achieves a peak value of 0.30 ± 0.01 then dramatically decreases to a steady-state value of 0.18 ± 0.02 associated with sample dilatancy. Under drained condition, the friction coefficient achieves peak values ranging from 0.28 ± 0.01 to 0.30 ± 0.01 , dramatically decreases to steady-state values of 0.21 ± 0.01 to 0.22 ± 0.01 , and then gradually re-strengthens with slip with sample compaction; (2) the slip-weakening distance D_c is varied from 2.03 ± 0.52 to 2.22 ± 0.49 under undrained and high-efficient-drainage conditions, respectively, to 1.14 ± 0.51 under less-efficient-drainage condition. After shearing, the color of kaolinite was changed from white to grey-dark color, and slicken-side textures were only observed on the slipping surface under drained condition. These results suggest that gouge was suffering frictional heat under drained condition, likely resulting from flash heating occurred on the slip surface.

Keywords: frictional behavior, fluid drainage, rotary shear, kaolinite, flash heating

Natural and experimental evidence of deformation on serpentinite

Wei-Hsin Wu¹、Li-Wei Kuo¹

(1)Department of Earth Sciences, National Central University

Serpentinite is regarded as a controlling factor for the nucleation and propagation of earthquakes within subduction zones. Recently, we have provided the evidence of deformation within serpentinite and nephrite from the paleo-subducting-origin Yuli Belt, Taiwan. However, the associated deformation conditions of which remain unclear. This study performs low-to-high velocity rotary shear (LHVR) rock friction experiments on water-saturated serpentinite gouges (sieved for grains size under 0.125mm) to investigate the frictional behaviour of incohesive serpentinite and the associated microstructures. All samples are deformed at either sub-seismic (0.001m/s) or seismic slip rates (1m/s) under both drained and undrained conditions at 10-MPa normal stress and ~5-m slip. Results show that the apparent friction coefficient μ is influenced by water drainage regardless of slip rates. For undrained condition, μ increased up to a peak value $\mu_p \sim 0.32-0.46$ and reached low steady-state value $\mu_{ss} \sim 0.2$, exhibiting a pronounced weakening behaviour explained by pore pressure rise. In contrast, under drained condition μ showed stable sliding ($\mu \sim 0.2-0.3$) or strengthening ($\mu > 0.2$) behaviour. Microanalytical methods, including optical microscope, field emission scanning electron microscope and in-situ synchrotron X-ray diffraction, will be utilized for the LHVR experimental products in near future. These mineralogical and microstructural results could provide a plausible mechanism for the obtained frictional behaviour. In particular, by integrating the recently reported deformation evidence of serpentinite, our results might help to determine the deformation modes within the serpentinite shear zones, and that the signatures of either transient frictional heating by propagation or pressure solution by creep were preserved in the studied serpentinite and nephrite of the Yuli belt.

Keywords: serpentinite, rotary shear, rock deformation, Yuli Belt

Raman spectroscopy and thermal conductivity of synthetic pyrope-grossular garnets at high pressure

Han-Yu Chen¹、Yun-Yuan Chang²、Pei-Ying Patty Lin¹、Wen-Pin Hsieh³、
Jennifer Kung⁴

(1)Department of Earth Sciences, National Taiwan Normal University、(2)Institute of Earth Sciences, Academia Sinica, Taiwan、(3)Institute of Earth Sciences, Academia Sinica, Taiwan; Department of Geosciences, National Taiwan University、(4)Department of Earth Sciences, National Cheng Kung University

Garnet is a major rock-forming mineral in the Earth's upper mantle and subducted slab. Knowledge of the thermal properties of silicate garnets is crucial to understand the thermal structure of the Earth's interior. The crystal structure of garnet can accommodate diverse elements. This study aims to investigate the compositional effects on the Grüneisen parameter and lattice thermal conductivity of pyrope (Py, $\text{Mg}_3\text{Al}_2(\text{SiO}_4)_3$)-grossular (Gr, $\text{Ca}_3\text{Al}_2(\text{SiO}_4)_3$) solid solution. The samples used in this study were synthetic single-crystal $\text{Py}_{40}\text{Gr}_{60}$ and grossular. High-pressure Raman spectroscopic measurements of samples were carried out using a diamond-anvil cell. The mode Grüneisen parameter for each observed Raman mode was obtained from the pressure dependence of vibrational frequencies. From the obtained mode Grüneisen parameters, we estimated the thermal Grüneisen parameters of our samples. Besides the Grüneisen parameters, we investigated the influence of Mg/Ca ratio on the lattice thermal conductivity of pyrope-grossular solid solution using time-domain thermoreflectance (TDTR) technique. Our experimental results will help to constrain the compositional effects on the heat flux and thermal structure in the Earth's interior.

Keywords: pyrope, grossular, solid solution, time-domain thermoreflectance, high pressures, lattice thermal conductivity

Crystallographic orientation-dependence of Raman mode behavior in ortho-(Mg, Fe) SiO₃ single-crystals under pressure

Sheng-Chih Chung¹、Florian T.S. Hua¹、Jennifer Kung¹

(1)Department of Earth Sciences, National Cheng Kung University

The major constructed unit for the pyroxene structure is the linkage of silicon-oxygen tetrahedrons (SiO₄) to form continuous chains. The chain structure reflects on the Raman pattern to be two strong paired Raman peaks (doublet) at the range of 660 and 1000 cm⁻¹, thereafter marked as ‘D1’ and ‘D2’, respectively. Previous Raman observations of pyroxenes indicated the doublet of 660 cm⁻¹ (D1) being sensitive to symmetry change, no matter induced by applied pressure or composition changed. In orthopyroxene, composition of (Mg, Fe) SiO₃, lately high pressure X ray diffraction studies showed that this series of pyroxene has a new high-pressure phase, HP P2₁/c. While the mentioned above phase transition occurred, the doublet of 660 cm⁻¹ (D1) would split into triplet from previous studies. Such observation has become a characteristic feature of symmetry changed from Pbca to HP P2₁/c. However, those observations were carried out either in powder form sample or unorientated single crystals. In order to investigate the detailed Raman mode feature of orthopyroxene across the phase transition, we measured the changes of the Raman modes, D1 and D2, along different major crystallographic axis, a, b c and face (210), up to 20 GPa. The composition of tested orthopyroxene ranges from Mg#100 to Mg#92, which the phase transition pressure of Pbca ® HP P2₁/c should be higher than 10 GPa. From a series of Raman measurement, we found the doublet splitting only observed on “c” axis. Moreover, in this study, both D1 and D2 were observed the splitting. Most strikingly the doublet splitting occurred as low as 4 GPa in which the pressure is far away from the phase transition defined by X ray diffraction. Our results raise the question if the doublet splitting in D1 and D2 can used as the sign of phase transition of orthopyroxene any longer. In this meeting we will report and discuss the observation in details.

Keywords: high pressure, Raman, pyroxene, phase transition

Rock physics parameters estimations of gas-hydrate and free gas concentrations in Formosa Ridge, Offshore SW Taiwan

Dipika Anggun Ardiantl¹、How-Wei Chen¹

(1)Department of Earth Sciences, Inst. of Geophysics, National Central University

Rock physics parameters usually can be estimated through well log-based analysis approaches with various proposed models and empirical equations. We propose a strategy which treat seismic data as a pseudo-log then combine post- and pre-stack modeling and inversion efforts for rock physics study. The approach helps to identify gas hydrate, free gas and its host lithology with fluids existence in Formosa Ridge Off., Southwestern Taiwan. We developed four steps workflow. First, we refined velocity model suggested from conventional NMO stack with semblance analysis. Second, the synthetic CMP gathers are created by reflectivity and convolutional approach respectively. If synthetic and real gather are fit in both offset domains, then confirms the estimated parameters. Third, initial impedance model derived from convolutional and reflectivity method are used separately in post- and pre-stack procedure. Once we have the P- S-impedance model and source wavelets extraction from offset-dependent dataset, then post- and pre-stack inversion were implemented sequentially to extract the best resolvable models. Pre-stack inversion based on three assumptions (a) linearized approximation for reflectivity, (b) angle-dependent Fatti's equation and (c) linear relationship among P-, S-impedance and density. The inferred basic parameters including V_p , V_s and density are the key efforts for further rock physics estimations. The parameters including porosity, bulk-shear modulus, resistivity, and water saturation for understanding the lithology conditions can be obtained through empirical equations. The results can assist us to evaluate the interrelationships among the derived parameters through cross-plots and delineate the potential gas hydrate and free gas concentration zones. The proposed approach enables us to obtain petro-physical properties with the hope that additional feasibility evaluation and confirmation from borehole data will be available in the future.

Keywords: seismic inversion, post-pre-stack, rock physics, gas-hydrate, free gas, pseudo-logs

Discretized Clay Shell Model (DCSM) of clayey Sandstone: Evaluating the effective stress coefficient of permeability

Pin-Lun Tai¹、Jia-Jyun Dong²

(1)Graduate Institute of Applied Geology, National Central University、(2)Graduate Institute of Applied Geology, National Central University; Earthquake-Disaster and Risk Evaluation and Management Center, National Central University

The effective stress coefficient determines the effective stress, which dominating the permeability of rocks. However, the documented value of for rocks shows a high scatter (0.3-5.5), based on the laboratory measurement. The well know Clay Shell Model (CSM) successfully explain why the effective stress coefficient of the clayey sandstone can well above 1 theoretically. However, CSM cannot account for the stress dependency of effective stress coefficient observed experimentally. In this study, a modification of CSM was proposed. This proposed Discretized Clay Shell Model (DCSM) discretizes multi-layers clay domain to account for the stress dependent elastic modulus of clay and calculates the pore radius of DCSM model under different confining stress and pore pressure. Iso-pore radius curves under different confining stress and pore pressure was used to determine the effective stress coefficient. The parametric study illustrates the superior features of the proposed DCSM to the traditional CSM. Critical findings include: (1) The predicted effective stress coefficient form a concaving upward surface in the pore pressure-confining stress space using DCSM. (2) The influence of pore pressure on effective stress coefficient will be stronger than the influence of confining stress especially under low pore pressure. (3) The predicted effective stress coefficient is not necessary positively or negatively correlated to confining stress under constant pore pressure. (4) The predicted effective stress coefficient for soft, high stress dependent deformability of clay coating on the pores of sandstones could be far higher than 1. Two synthetic cases (laboratory and in-situ scale) illustrate the importance of stress dependent effective stress coefficient for determining the effective stress and permeability.

Keywords: permeability, effective stress coefficient, clayey sandstone

Petro-physical properties identification of gas hydrate and free-gas in Yuan-An Ridge, southwest Taiwan

Dwi Ayu Karlina¹、How-Wei Chen¹

(1)Department of Earth Sciences, National Central University

Hydrate and free gas existence in the unconsolidated marine sediments produce significantly large effect on the elastic properties changes in Yuan-An Ridge. Simultaneous Prestack Inversion (SPI) were used to distinguish the physical properties changes. SPI use conjugate gradient matrix inversion method in junction with computing angle-dependent reflectivity responses which follows Fatti's equation. Hence, quality control on SPI result by comparing synthetic to real data in angle gather is very important. SPI has two assumptions. First, the constant ratio of S-wave velocity over P-wave velocity within a rock layer and the background trend should corresponds to wet clastic. V_p/V_s ratio is later converted to natural logarithm P-Impedance (Z_p) and S-Impedance (Z_s). Second, based on Gardner equation, natural logarithm of density has linear relationship with P-impedance. Hence, the synthetic responses is computed by reflectivity method defined by the combined effects from P-impedance, S-Impedance, and density. Consequently, the elastic properties including V_p , V_s , density, Z_p , Z_s , V_p/V_s ratio can be obtained. Other associate elastic properties such as P-wave modulus, shear modulus, Young modulus, Bulk modulus, Poisson's Ratio, $\lambda\rho$, and $\mu\rho$ can be derived through known models and its corresponding equations. The parameters to characterize gas hydrate and free gas in unconsolidated marine sediment can be derived through the approach demonstrated. Parameters which are very sensitive to the gas hydrate and free gas existence in Yuan-An Ridge are $\lambda\rho$, and $\mu\rho$. They can be separated from background trend through cross plot.

Keywords: elastic properties, free gas, Fatti's equation, gas hydrate, and incident angle

Toward a realistic lattice solid model for earthquake micro-physics and earthquake cycle simulation

How-Wei Chen¹

(1)Department of Earth Sciences, National Central University

A realistic numerical simulation model for all physical processes underlying the earthquake phenomenon on HPC's would provide a powerful tool to study fault behavior and earthquake nucleation. The microphysical particle-based Lattice Solid Model (LSM) currently being developed at QUAKES provides a basis on which to construct such a model. Presently, the model simulates stress transfer, seismic waves, fracture, friction, heat and gouge dynamics. Simulations show numerous features compatible with laboratory and field studies including shear localization, low-strength faults compatible with the Heat-Flow Constraint, slip pulses on faults, Gutenberg-Richter power law statistics and cycles of seismic activity exhibiting accelerating energy release prior to large events. Ultimately, when fully developed, it is envisaged that the LSM will be capable of simulating all physical processes underlying earthquakes including lubrication and dynamics of fluids, phase transformations, and chemical effects as well as all observable signals including strain, seismic, electric and magnetic. Increased computational capacity, a model refinement process involving feedback with laboratory and field observations, and integration with macroscopic simulation models would provide the means to study the earthquake cycle, and hence, to develop earthquake hazard quantification and forecasting methodology that best uses the incomplete recorded and incoming data. Recent LSM simulation results of patterns of accelerating energy release prior to large events suggest that earthquake statistics can evolve in a predictable way. These results demonstrate the potential utility of realistic numerical simulation models as a means to probe the earthquake cycle, and provide encouragement that earthquake forecasting is feasible, at least under certain conditions.

Keywords: Lattice Solid Model, rupture simulation, micro-physics, earthquake cycle